

J
② LEVEL II

AFML-TR-79-4196

ADA 086671

A REVIEW OF NONLINEAR FRACTURE
MECHANICS RELATIVE TO FATIGUE

T. Weerasooriya
J. P. Gallagher
H. C. Rhee

University of Dayton Research Institute
300 College Park Drive
Dayton, Ohio 45469

SEPTEMBER 30, 1979

TECHNICAL REPORT AFML-TR-79-4196
Final Report for Period September 1978 - September 1979

Approved for public release; distribution unlimited

AIR FORCE MATERIALS LABORATORY
AIR FORCE WRIGHT AERONAUTICAL LABORATORIES
AIR FORCE SYSTEMS COMMAND
WRIGHT-PATTERSON AFB, OHIO 45433

S DTIC ELECTE D
JUL 11 1980
B

FILE COPY

NOTICE

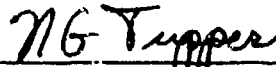
When Government drawings, specifications, or other data are used for any purpose other than in connection with a definitely related Government procurement operation, the United States Government thereby incurs no responsibility nor any obligation whatsoever; and the fact that the government may have formulated, furnished, or in any way supplied the said drawings, specifications, or other data, is not to be regarded by implication or otherwise as in any manner licensing the holder or any other person or corporation, or conveying any rights or permission to manufacture, use, or sell any patented invention that may in any way be related thereto.

This report has been reviewed by the Information Office (OI) and is releasable to the National Technical Information Service (NTIS). At NTIS, it will be available to the general public, including foreign nations.

This technical report has been reviewed and is approved for publication.



THEODORE NICHOLAS
Project Engineer



NATHAN G. TUPPER, Chief
Metals Behavior Branch
Metals and Ceramics Division

If your address has changed, if you wish to be removed from our mailing list, or if the addressee is no longer employed by your organization please notify _____, W-PAFB, OH 45433 to help us maintain a current mailing list.

Copies of this report should not be returned unless return is required by security considerations, contractual obligations, or notice of a specific document.

UNCLASSIFIED
SECURITY CLASSIFICATION OF THIS PAGE (When Data Entered)

19 REPORT DOCUMENTATION PAGE		READ INSTRUCTIONS BEFORE COMPLETING FORM
1. REPORT NUMBER	2. GOVT ACCESSION NO.	3. PRICE PER COPY (Catalog Number)
AFML TR-79-4196	AD-A086671	Final
4. TITLE (and Subtitle)	5. PERFORMING ORG. REPORT NUMBER	6. AUTHOR(s)
A Review of Nonlinear Fracture Mechanics Relative to Fatigue.	UDR-TR-79-98	T. Weerasooriya, J.P. Gallagher, H.C. Rhee
7. AUTHOR(s)	8. CONTRACT OR GRANT NUMBER(s)	9. PERFORMING ORGANIZATION NAME AND ADDRESS
T. Weerasooriya, J.P. Gallagher, H.C. Rhee	F33615-78-C-5184	University of Dayton Research Institute Dayton, Ohio 45469
10. CONTROLLING OFFICE NAME AND ADDRESS	11. NUMBER OF PAGES	12. SECURITY CLASS. (of this report)
Air Force Materials Laboratory Air Force Systems Command Wright-Patterson AFB, Ohio 45433	76	Unclassified
14. MONITORING AGENCY NAME & ADDRESS (if different from Controlling Office)	15. SECURITY CLASS. (of this report)	15a. DECLASSIFICATION DOWNGRADING SCHEDULE
	Unclassified	
16. DISTRIBUTION STATEMENT (of this Report)		
Approved for public release; distribution unlimited.		
17. DISTRIBUTION STATEMENT (of the abstract entered in Block 20, if different from Report)		
18. SUPPLEMENTARY NOTES		
19. KEY WORDS (Continue on reverse side if necessary and identify by block number)		
20. ABSTRACT (Continue on reverse side if necessary and identify by block number)		
The report reviews currently available parameters, methodology, and data that support further developments in elastic-plastic fracture mechanics (EPFM) technology for modeling fatigue crack growth rate (FCGR) behavior. In general, it can be stated that linearly elastic fracture mechanics (LEFM) parameters can be used to model FCGR behavior except when the zone of cyclic plasticity accompanying the crack process is large with respect		

DD FORM 1473 JAN 73 EDITION OF 1 NOV 65 IS OBSOLETE

UNCLASSIFIED
SECURITY CLASSIFICATION OF THIS PAGE (When Data Entered)

105400

mt

UNCLASSIFIED

SECURITY CLASSIFICATION OF THIS PAGE (When Data Entered)

7 to crack length and other structural length parameters. The literature provides two types of EPFM parameters which are available for modeling FCGR behavior when the limitations of LEFM are exceeded: one type is based on the characterization of the intensity of the crack tip stress-strain field, the other is based on the determination of a specific mechanical parameter which is evaluated at a point close to the crack tip.

UNCLASSIFIED

SECURITY CLASSIFICATION OF THIS PAGE (When Data Entered)

FOREWORD

This Technical Report was prepared by the Aerospace Mechanics Division of the University of Dayton Research Institute for the Metals and Ceramics Division, Air Force Materials Laboratory. Dr. T. Nicholas, AFML/LLN is the project engineer. This work covers the completion of Task I of the Contract F33615-78-C-5184, "Nonlinear Fracture Mechanics," (Work Unit Number-24180306), and is part of the work conducted on the above contract from September 1978 to September 1979.

The authors wish to express their appreciation for the careful review of this report to Dr. T. Nicholas of AFML/LLN and Dr. A.F. Grandt, Jr., formerly of AFML/LLN. The authors also wish to thank Dr. J. Ahmad of SRL for review of the finite element section of this report.

DTIC
ELECTE
S JUL 11 1980 D
B

ACCESSION for		
NTIS	White Section	<input checked="" type="checkbox"/>
DDC	Buff Section	<input type="checkbox"/>
UNANNOUNCED		<input type="checkbox"/>
JUSTIFICATION _____		
BY _____		
DISTRIBUTION/AVAILABILITY CODES		
Dist.	AVAIL.	and/or SPECIAL
A		

TABLE OF CONTENTS

SECTION		PAGE
I	INTRODUCTION	1
	1.1 Background and Scope	1
	1.2 The Breakdown of LEFM	2
	1.2.1 The LEFM Approach to Fatigue	2
	1.2.2 High-FCGR Nonlinear Behavior	6
	1.2.3 Nonlinear Behavior at Notches	9
	1.3 Summary of Nonlinear Behavior	11
II	NONLINEAR FRACTURE MECHANICS PARAMETERS	14
	2.1 The Field Approach	14
	2.1.1 Derivatives of Elastic Fields	15
	2.1.2 Elastic-Plastic Field Parameters	19
	2.2 Crack Tip Approach	24
	2.2.1 Crack Tip Parameters	26
	2.2.1.1 Near Tip Strain Parameter	26
	2.2.1.2 Crack Tip Opening Displacements and Angles	27
	2.2.1.3 Crack-Tip Node Force (F)	30
	2.2.2 Energy-Based Parameters	30
	2.3 Evaluation of EPFM Parameters	32
	2.3.1 Crack Tip Analysis by Finite Elements	34
	2.3.1.1 Crack Tip Singularity Modeling	34
	2.3.1.2 Crack Tip Blunting	35
	2.3.2 Numerical Estimation of the J-Integral	38
	2.2.3 Concluding Remarks on Finite Element Results	39
III	SUMMARY OF AVAILABLE DATA	42
	3.1 The FCGR LEFM Parameter Correlations	42
	3.1.1 Stress Intensity Factor Correlations	42
	3.1.2 Strain Intensity Factor	47

TABLE OF CONTENTS (Concluded)

SECTION		PAGE
III	3.2 J-Integral Parameters	48
	3.2.1 Operational J-Techniques - Summary	48
	3.2.2 Operational J-Data Summary	53
	3.3 Other FCGR Correlations	62
	3.4 The Methodology, the Approaches, and Some Issues	62
	3.4.1 Life Estimation Scheme Using EPFM Approach	65
	3.4.2 Summary	66
IV	RECOMMENDATIONS	68
	REFERENCES	69

LIST OF ILLUSTRATIONS

FIGURE		PAGE
1	Schematic Illustrating FCGR Data Reduction Approach Based on the LEFM Parameter, K_{max} . The Maximum Stress Intensity in a Stress Cycle (Reference 1).	3
2	Schematic Illustrating How the FCGR Database is used in Conjunction with a Structural Analysis Based on LEFM Methodology to Predict the Crack Growth Behavior for Structural Crack Geometries (Reference 1).	5
3	FCGR-LEFM Curve for Complete Range of Observed Behavior.	7
4	LEFM ΔK Parameter Correlation with FCGR Data for 2024-T3 Aluminum Alloy (Reference 5).	8
5	LEFM ΔK Parameter Correlations with FCGR Data for Man-Ten Steel (Reference 6); the parameter ΔK is Defined as $K_{max} - K_{min}$, where $K_{min} = \sigma_{min} \cdot (K/\sigma)$. The Data were Generated using WOL Specimens.	10
6	Plastic and Elastic Fracture Mechanics Characterization of Fatigue Crack Growth (Reference 7).	12
7	Elastic-Stress-Field Distribution Ahead of Crack (Reference 9).	16
8	Distribution of the σ_y Stress Component in the Crack-Tip Region (Reference 9).	18
9	Linear-Elastic Crack-Tip Stress and Strain Fields (Reference 13).	19
10	Crack-Tip Stress and Strain Fields Surrounding the Crack (Reference 13).	20
11	Expanded View of the Elastic-Plastic Stress-Strain Field (Reference 13).	20
12	Crack Tip Displacement Related Parameters Two Definitions of Crack Opening Angle and Displacement.	28
13	Generalized Energy Release Rate (G).	33
14	Undeformed Configuration of Finite Element Mesh for the Notch-Blunting Solution (Reference 58).	37

LIST OF ILLUSTRATIONS (Concluded)

FIGURE		PAGE
15	Finite Element Mesh for Crack Tip Blunting (Reference 39).	39
16	Crack Mouth Opening Displacement as a Function of Magnitude of Applied Load (Reference 60).	40
17	Dubensky's 2024-T3 FCGR Data Presented as a Function of K_{\max} for the Three Highest Levels of Maximum Gross Stress.	44
18	Correlation of "High" FCGR and Monotonic Tearing Behavior with LEFM Parameter K_{\max} ($=K_R$).	46
19	Fatigue Crack Growth Rate Versus Cyclic J for Various Geometries (Reference 71).	49
20	Procedure for Calculating Operational Values of the J-Integral.	51
21	A Schematic Description of the Two Approaches Used to Determine Operational Values of the J-Integral - After Reference 74.	52
22	Estimation of Small Crack ΔJ from Stress Strain Hysteresis Loops (Reference 72).	54
23	Comparison of Small Crack Data with Scatterband from Test Results for Ordinary and Large-Size Specimens (Reference 72).	55
24	Fatigue Crack Growth Rates as a Function of Modified ΔJ . (Reference 8).	56
25	Crack Growth Data in Terms of ΔJ Determined Using the Merkle-Corten Approximation (Reference 74).	57
26	Schematic Representation of Initial Loading Cycles (Reference 81).	60
27	High-Strain Fatigue Crack Propagation Rates as a Function of Crack Opening Displacement. Tests Carried out at 20°C and 300°C in repeated Tension on Mild Steel Plates 1.83m x 0.91m x 12.7mm Containing a Central Sharp 0.23m slit (Reference 82).	63
28	Crack Growth Data in Terms of Load-Line Displacement Parameter (Reference 74).	64

SECTION I
INTRODUCTION

1.1 BACKGROUND AND SCOPE

In the mid 1950's, a new concept for characterizing the fracture behavior of materials evolved from studies of the stress field at the tip of a crack in an elastic body. It was quickly noted that a single parameter, the stress intensity factor (K), incorporated the influence of remote stress, crack length, and structural geometry. This parameter was successfully used to correlate the conditions associated with the initiation of fracture between service structures and laboratory test specimens manufactured from high strength metals. By the early 1960's, this same concept was found to provide an acceptable procedure for correlating fatigue crack growth rate behavior between cracks of different configurations subjected to various loading conditions. The approach to describing fracture and fatigue crack growth rate behavior based on the stress intensity factor has sometimes been referred to as the fracture mechanics approach, but more specifically and recently as the linear elastic fracture mechanics (LEFM) approach.

The LEFM approach basically follows a similitude approach where the identical local stress-strain behavior and resulting crack growth behavior are assumed to occur for all cracks having the same stress intensity factor. It is realized that ordinary structural materials do not exhibit complete elastic behavior, especially in the crack tip region. However, if the zone of nonlinear deformation is small and contained in the elastic stress field, the elastic stress field will set the boundary conditions for the deformation of the material in the nonlinear zone. Hence, the LEFM approach will describe fracture and fatigue crack growth rate behavior as long as the nonlinear deformation zone at the crack tip is small enough so that the surrounding elastic stress field can be described by the elastic stress intensity factor.

Since 1970, an ever increasing amount of attention has been given to defining the limitations of the widely used LEFM approach. Most of this attention is devoted to improving the characterization of the onset of monotonic cracking behavior and the subsequent slow stable tearing that precedes the fracture of ductile materials (of the type that might be found in nuclear power plant systems). More recently, loading and/or material conditions have been noted to limit the LEFM parameter K 's ability to correlate the fatigue crack growth rates generated using (a) different types of laboratory specimen geometries and (b) different stress-crack length combinations within the same specimen geometry. Unfortunately, the conditions that cause the normally good fatigue crack growth rate (FCGR) correlations (based on the LEFM approach) to breakdown are not particularly well documented. Typically, when the FCGR-LEFM correlations are noted to breakdown, the resulting behavior is referred to as nonlinear fracture mechanics behavior. This terminology, however, has led to even further communication problems.

This report has been written in an attempt to clarify the limitations of the FCGR-LEFM methodology and to review alternate approaches which have the potential for improving the characterization of FCGR behavior. Additionally, the report provides: (1) a review of currently available elastic-plastic fracture mechanics (EPFM) parameters that might improve FCGR correlations, (2) a summary of available data that exhibit a lack of correlation based on the LEFM approach, and (3) a recommended course of action for investigating parameters that have the potential to provide for improved FCGR correlations.

1.2 THE BREAKDOWN OF LEFM

1.2.1 The LEFM Approach to Fatigue

To clarify the limitations in the LEFM approach, we will initially provide an overview-type review of the FCGR-LEFM methodology. Shown in Figure 1 is a schematic which describes the procedure by which fatigue crack growth (FCG) data are collected in the laboratory, reduced to FCGR data, and subsequently

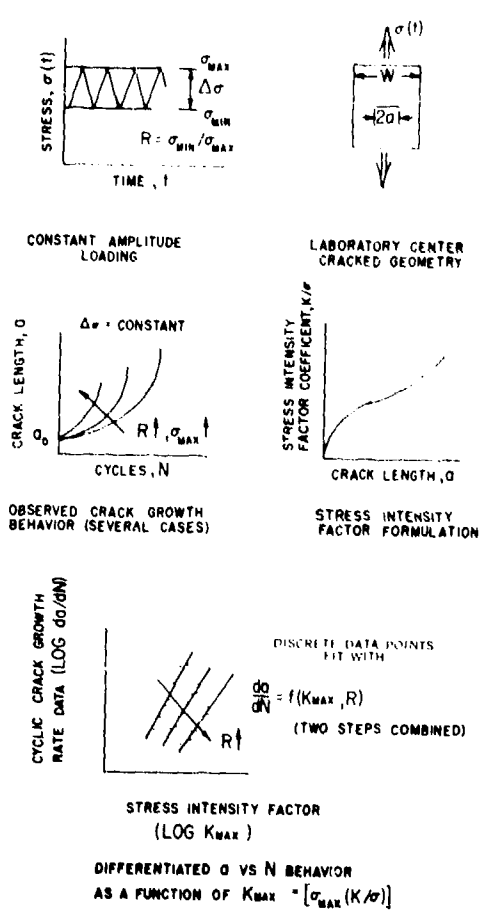


Figure 1. Schematic Illustrating FCGR Data Reduction Approach Based on the LEFM Parameter, K_{max} . The Maximum Stress Intensity in a Stress Cycle (Reference 1).

portrayed as a function of the LEFM parameter K . To summarize the approach, FCG data are collected under constant amplitude stress cycling histories at various stress ratios using a well characterized structural geometry, i.e. characterized with respect to the crack driving parameter. The FCG data are reduced using standardized numerical techniques and presented as a function of the LEFM crack driving parameter.

Various authors choose to use K_{\max} , the maximum value of the stress intensity factor (SIF) in a cycle of loading, or ΔK , the SIF range (maximum minus minimum SIF) as the LEFM parameter. ASTM Subcommittee E24.04 on "Subcritical Crack Growth" has adapted ΔK as the parameter that will be used in portraying FCGR data generated according to the new ASTM Standard E647-78T.

The usefulness of the FCGR-LEFM data comes from the observation that these data are independent of both structural geometry (including crack size) and stress level. In fact, this independence is the basic hypothesis underlying what is referred to as the fracture mechanics approach. Numerous instances, where the FCGR-LEFM modeling approach has been suggested to fail, have resulted from less than accurate characterizations of the SIF; this is particularly the case when one attempts to model 3-D flaws in stress concentration regions with gross estimates of the SIF.

As suggested by Figure 2, the process of numerical differentiation of FCG data is reversed when one desires to obtain a life prediction for a structural component which contains a crack. The final verification for any life prediction scheme comes when life predictions are made for conditions (stress level, stress ratio, structural geometry, etc.) for which the test life is not known a priori to the analyst; this is normally referred to as making a "blind" life prediction. In general, FCG blind life predictions within plus or minus twenty (20) percent of the observed test life are considered good while those that differ by more than a factor of two (2) are considered poor.

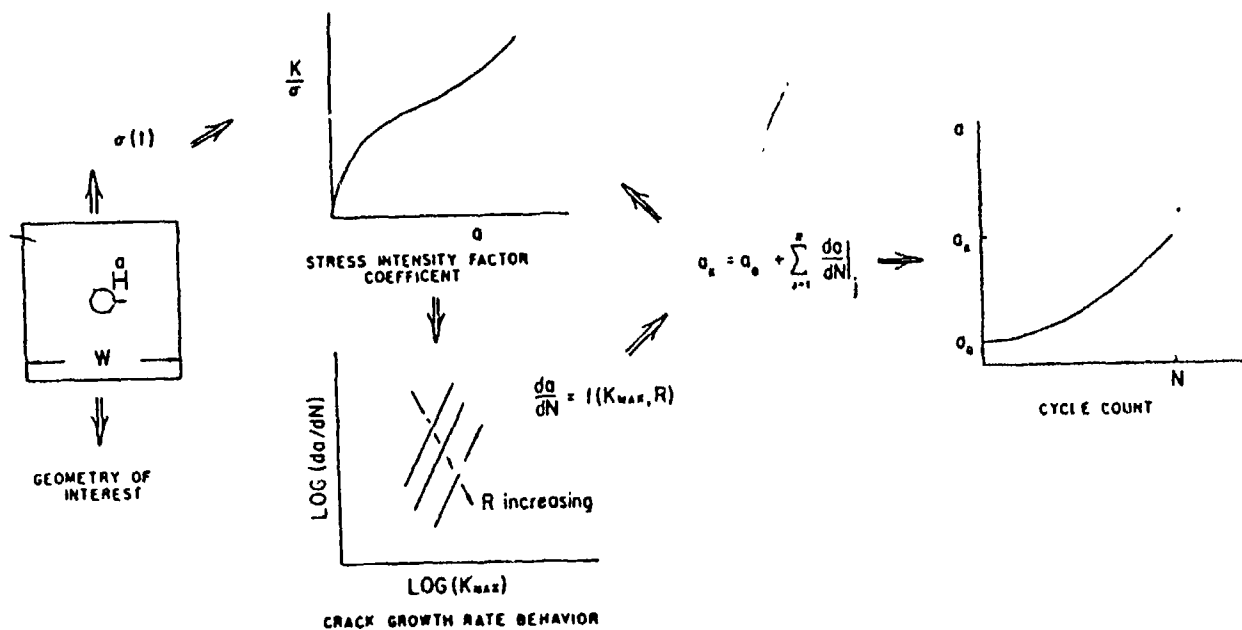


Figure 2. Schematic Illustrating How the FCGR Database is used in Conjunction with a Structural Analysis Based on LEM Methodology to Predict the Crack Growth Behavior for Structural Crack Geometries (Reference 1).

1.2.2 High-FCGR Nonlinear Behavior

Assuming that the LEFM approach applies, material engineers can expect the FCGR data generated using any well characterized (cracked) structural geometry to always scatter closely about the mean FCGR behavior curve established from data collected using any other well characterized structural geometry. One of the initial definitions of what might be called nonlinear fracture mechanics behavior arose as a result of portraying FCGR data scattered around a power law equation, attributed to Paris², and having the form:

$$\frac{da}{dN} = C(\Delta K)^n \quad (1)$$

which describes a straight line in log-log coordinates. A set of power law equations, in terms of K_{max} can be seen expressed in Figures 1 and 2. Figure 3 provides a complete representation of FCGR data for a single stress ratio (R) that fully illustrates the shape that a FCGR-LEFM curve assumes. As the reader will note, a power law equation will have its greatest utility in the central region of the FCGR-LEFM curve. Barsom³, in considering the strain energy release rate ($\Delta G = \Delta K^2/E$) approach to fatigue, observed that deviations from the power law relation, which he termed "nonlinear behavior", could be anticipated on the basis of a crack opening displacement (COD) parameter. Barsom used LEFM methodology to estimate the controlling COD parameter from the SIF and was not strictly interested in the limitations of LEFM.

Additional investigators who have also studied FCGR behavior above the "power law" region of the FCGR-LEFM curve have noted that FCGR behavior is not always uniquely related to the LEFM driving parameter. Frost et al.⁴ have presented previously published FCGR data as a function of ΔK which demonstrate that the maximum applied stress (or net section stress) will influence the FCGR behavior in the High-FCGR region for some but not all metals studied. Dubensky⁵, in his analysis of 7075 and 2024 aluminum alloys in the High-FCGR region, has noted a controlling effect of the maximum applied stress on the 2024 behavior (See Figure 4)

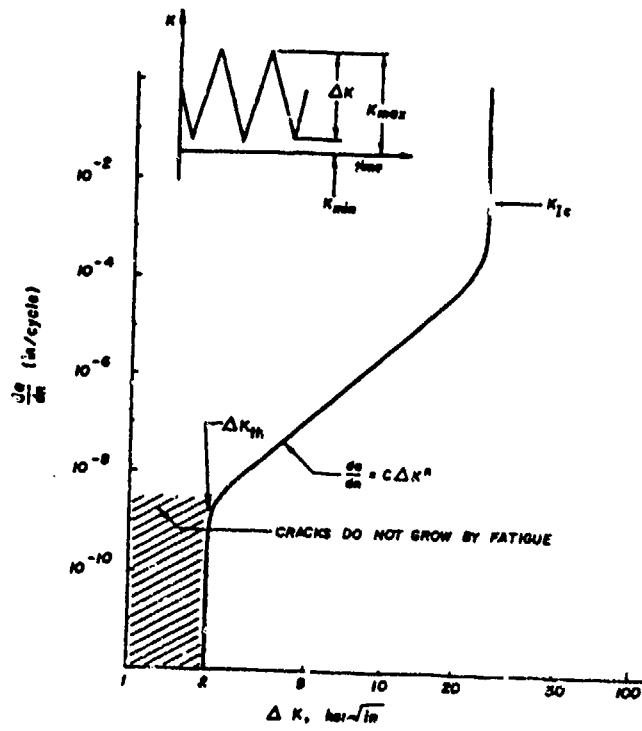


Figure 3. FCGR-LEFM Curve for Complete Range of Observed Behavior.

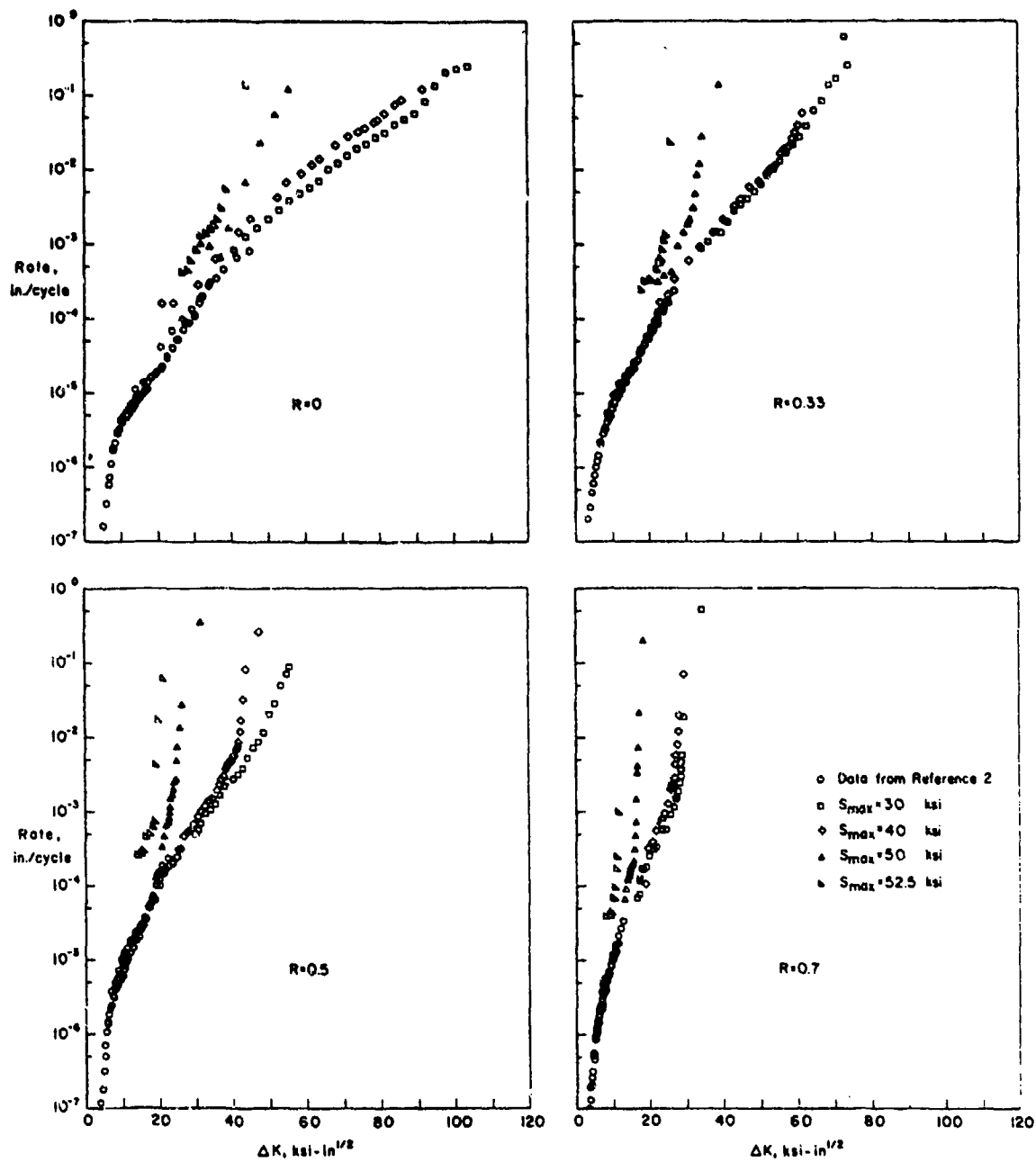


Figure 4. LEFM- ΔK Parameter Correlation with FCGR Data for 2024-T3 Aluminum Alloy (Reference 5).

but not on the 7075. Dowling and Walker⁶ have presented data for two relatively low strength steels, Man-Ten and RQC-100. They have noted evidence for stress or crack length effects only in the High-FCGR region in the lower strength Man-Ten steel as shown in Figure 5. While at this time it can not be stated absolutely, it does appear that the FCGR behavior of the more ductile alloys exhibit an effect of maximum stress in the High-FCGR region, thus violating a basic premise of the LEFM approach to fatigue. For the brittle alloys, this effect may not be observed because fracture takes place before the plastic-zone can grow to a size that invalidates the LEFM assumptions of contained plasticity. Frost et al.⁴ attempt to qualify the usefulness of LEFM by setting a limit on the plastic zone size (r_y) in a center-cracked (CC) or edge-cracked (EC) test specimen:

$$r_y = \frac{1}{2\pi} \left(\frac{K_{\max}}{\sigma_0} \right)^2 \leq \frac{a}{7} \quad (2)$$

where σ_0 is the yield strength and a is the half-crack length in the CC specimen and the crack length in the EC specimen. While Frost et al. support their hypothesis with High-FCGR observations for a number of materials, their testing programs were not designed to validate the use of Equation 2 as an absolute condition for applying the LEFM approach.

1.2.3 Nonlinear Behavior at Notches

The material at the root of a notch in a highly loaded structure does not need to contain a pre-existing defect to experience fatigue cracking problems. When the level of cyclic plastic deformation is consistently high, a crack will initiate and subsequently grow under the influence of this deformation. Hammouda and Miller⁷ have recently provided a clear description of the expected FCGR behavior in notch regions when the level of cyclic loading induces relatively large local plastic deformation. They accurately point out that LEFM technology is invalid here because the crack is imbedded within a plastic stress-strain field and not an elastic stress field generated by the moving crack.

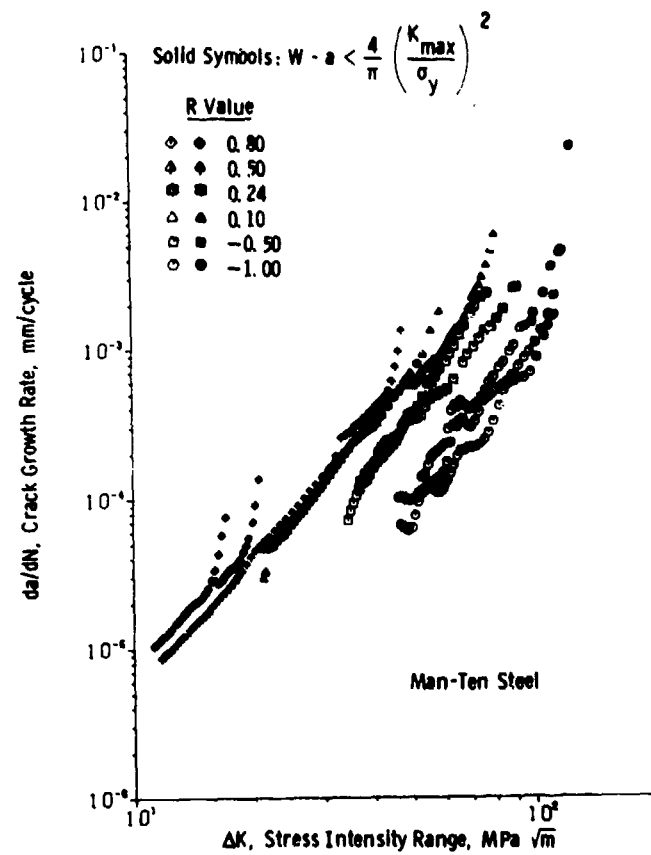


Figure 5. LEFM- ΔK Parameter Correlations with FCGR Data for Man-Ten Steel (Reference 6); The Parameter ΔK is Defined as $K_{max} - K_{min}$, where $K_{min} = \sigma_{min} \cdot (R/\sigma)$. The Data Were Generated Using WOL Specimens.

Figure 6 portrays the FCGR pattern observed by the small cracks initiated by and embedded within the cyclic plastic stress-strain field at the root of a notch. As the figure shows, a crack first grows at rapid rates and as its length increases, the rate of growth decreases until the behavior becomes controlled by the assumptions of LEFM. Based on a modification suggested by El Haddad et al.⁸, it may be possible to distinguish between cracks that can be modeled using a stress-strain field parameter such as the J-Integral and those that might require parameters that are beyond those currently available.

1.3 SUMMARY OF NONLINEAR BEHAVIOR

The correlation of FCGR with the single LEFM parameter appears to fail for those conditions in which the crack is either propagating into or through a zone of gross plastic yielding (Figures 4-6). When a crack is propagating through a material experiencing net section yielding, material ratcheting will further increase the levels of crack tip strain fields above that predicted by LEFM. In these cases, the crack no longer generates an elastic stress field which contains and controls the cyclic behavior of the nonlinear material at the tip of the crack.

To better describe FCGR response under loading conditions which induce nonlinear material behavior, a number of investigators have suggested the use of Elastic-Plastic Fracture Mechanics (EPFM) parameters. These parameters are based on either the field approach or the crack tip approach. The field approach follows that of the LEFM approach in that a parameter is used that can be related to the intensity or magnitude of the response-controlling elastic-plastic stress-strain field at the tip of a crack. The crack tip approach is based on a philosophy, whereby one determines the value of the parameter at the crack tip which is suspected of controlling the crack/growth behavior. When EPFM parameters are used to describe the fatigue and fatigue crack growth behavior, the approach is normally referred to as the nonlinear fracture mechanics (NLFM) or elastic-plastic fracture mechanics (EPFM) approach; its characterizing parameter is referred to as the NLFM or EPFM parameter.

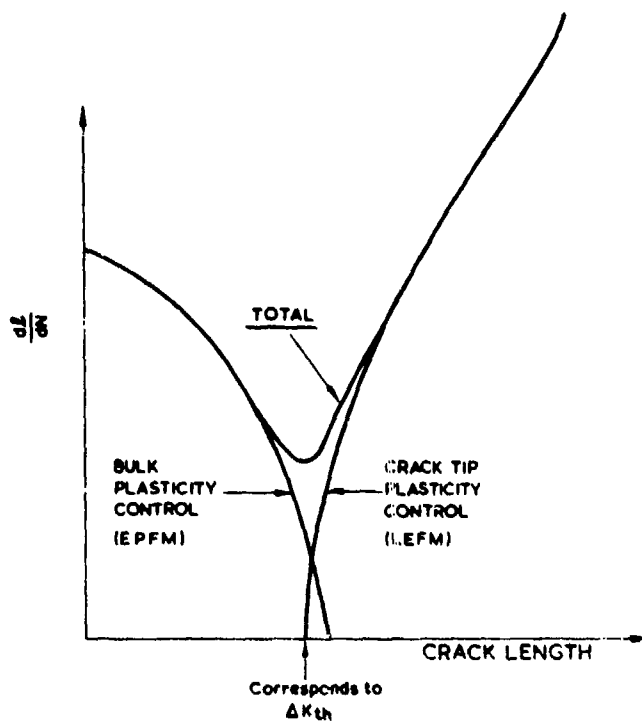


Figure 6. Plastic and Elastic Fracture Mechanics Characterization of Fatigue Crack Growth (Reference 7).

In the sections that follow, we will review currently available EPFM parameters and FCGR data which support the development of a FCGR-EPFM methodology along the lines suggested by Figures 1 and 2 where K_{max} is replaced with an EPFM parameter "P". The basic restriction of such a development is that the FCGR-EPFM curve, once established, will be independent of both the level of applied cyclic stress and structural geometry (including crack length).

SECTION II

NONLINEAR FRACTURE MECHANICS PARAMETERS

A survey of potentially useful parameters applicable for FCGR correlations has shown that the available parameters can be divided into two categories:

- (1) those that characterize the intensity of an elastic-plastic stress-strain field, and
- (2) those that characterize the magnitude of a suspected controlling parameter at a point located at or near the crack tip.

This section identifies the parameters by category and provides the background associated with the development of these parameters. Most of the parameters identified in this section have only been used so far in the monotonic fracture loading situations. Also, currently available numerical techniques for evaluating some of these parameters are reviewed.

2.1 THE FIELD APPROACH

There are a broad class of parameters which have evolved from analytical studies of the crack tip stress and strain fields. The analytical continuum mechanics studies have shown that single parameter characterizations of the stress-strain field at a crack tip are possible as long as these fields are not distorted by gross plastic deformation. It is recognized that these stress-strain fields do not extend directly into the intensely distorted localized region at the crack tip, where the deformation processes are controlling the observed crack growth behavior. However, since the intensely distorted localized region is imbedded within a less intense but definable stress-strain field, it is argued that the less intense stress-strain field provides the boundary conditions that control the deformation processes within the intensely distorted zone. Thus, if the parameter which establishes the magnitude of the less intense stress-strain field can be determined, it can be utilized via a similitude hypothesis to characterize the behavior of cracks.

This subsection will identify the currently available field parameters. Table 1 provides a listing of those parameters which have been used to characterize the intensity of the crack tip stress-strain field. Several LEFM derivatives are presented in the table for completeness.

TABLE 1

NONLINEAR FRACTURE MECHANICS FIELD PARAMETERS

<u>Elastic Field Derivatives</u>	<u>Symbol</u>
Stress Intensity Factor (SIF)	$K = \sigma\beta\sqrt{\pi a}$
Plasticity Corrected SIF ($a^*=a+r_y$)	$K = \sigma\beta\sqrt{\pi a^*}$
Strain Intensity Factor	$K_\epsilon = \epsilon\beta\sqrt{\pi a}$
Neuber Intensity Factor	$K_N = \sqrt{K \cdot K_\epsilon E}$
 <u>Elastic-Plastic Fields</u>	
J-Integral	J
Crack Tip Opening Displacement (CTOD)	δ_t

2.1.1 Derivatives of Elastic Fields

With the success of LEFM in predicting extension of cracks in elastic materials, researchers have been considering the extension of LEFM to the elastic-plastic regime.

Figure 7 shows the elastic-stress-field distribution ahead of the crack tip^{10,11}. When there is no plasticity (a case which does not exist for real materials) the Mode I crack opening stress σ_y is proportional to the stress intensity factor (SIF), K_I , in the vicinity of the crack tip. The stress-field equations show that the distribution of the elastic-stress field in the vicinity of the crack tip is invariant in all structural components subjected to this type of deformation, and that the single parameter K_I describes the intensity of crack tip stress and strain field. The rationale in using the stress intensity factor to describe FCGR behavior follows from the ability of the elastic stress-strain field to control the deformation behavior in the

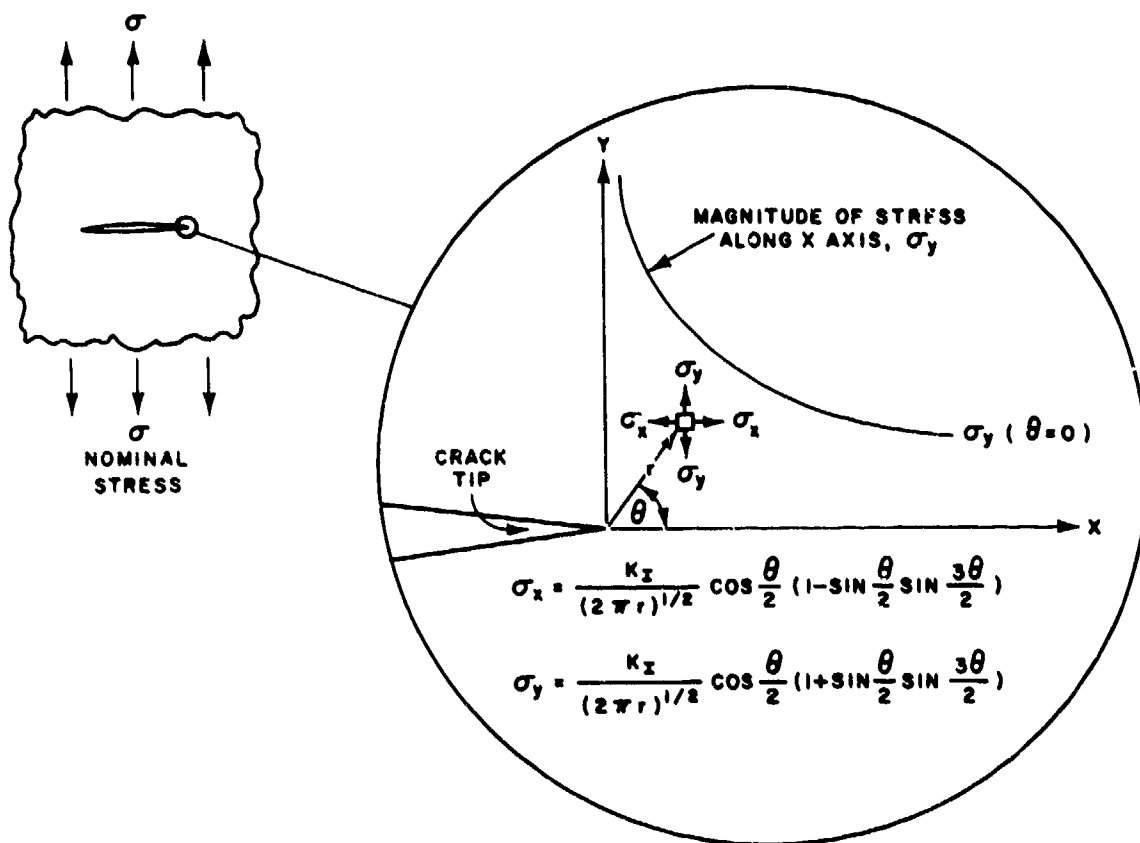


Figure 7. Elastic-Stress-Field Distribution Ahead of Crack (Reference 9).

distorted crack tip zone under cyclic loading. This same rationale holds for the strain intensity factor (K_{ϵ}).

In metals, stresses at the crack tip are finite and plastic yielding occurs at the crack tip. A schematic illustrating the distribution of the stress normal to the path of the crack is shown in Figure 8. The extent of the yielding ahead of the crack tip can be estimated as twice the Irwin plastic zone size (r_y) which is given by:

$$r_y = \frac{1}{2\pi} \left(\frac{K_I}{\sigma_0} \right)^2 \quad (3a)$$

for plane-stress conditions and

$$r_y = \frac{1}{6\pi} \left(\frac{K_I}{\sigma_0} \right)^2 \quad (3b)$$

for plane-strain conditions. Irwin¹² suggested that an increase in the real crack length r_y (See Figure 9)¹³ will result in a modified crack which has an elastic stress distribution similar to the elastic-field-stress distribution in the vicinity of the real crack's plastic zone boundary. Therefore, when the amount of yielding at the crack tip is limited, attempts have been made to use LEFM parameters, corrected to account for the plasticity, to modeling FCGR behavior. In addition to the plastic zone correction suggested by Irwin, there exist other corrections by Dugdale¹⁴ and Newman¹⁵.

Attempts to model FCGR behavior using plasticity modified SIF for elastic-plastic or fully-plastic material behavior have had only modest success. The reason for the limited success results from the fact that when the plastic zone size is appreciably large, (larger than the K-field; zone 1 in Figure 9) the stress-field in the vicinity of the crack tip is not predicted accurately by the elastic solution. Thus, for more generality and accuracy one must proceed to an elastic-plastic analysis; that is, to consider the vicinity of the crack tip as an elastic-plastic or fully plastic field.

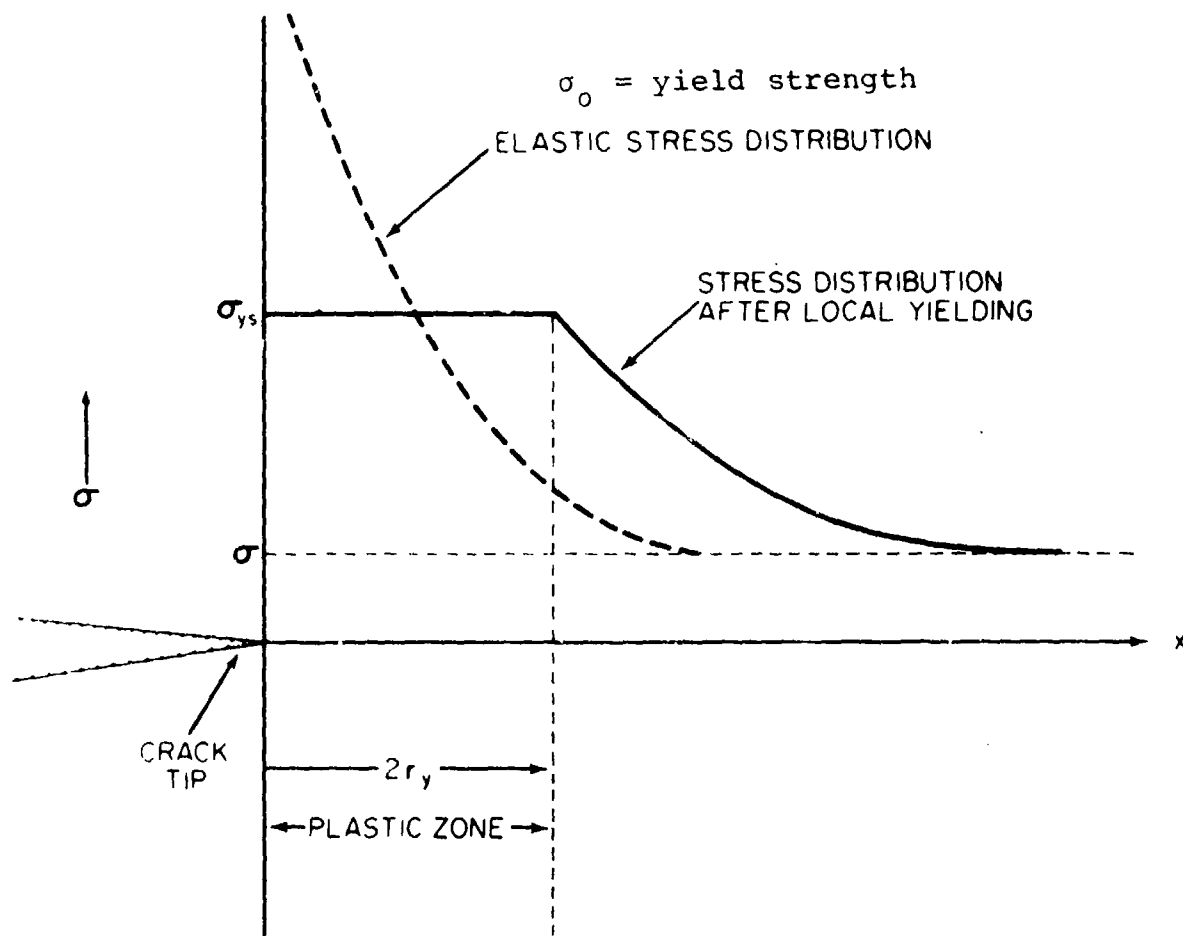


Figure 8. Distribution of the σ_y Stress Component in the Crack-Tip Region (Reference 9).

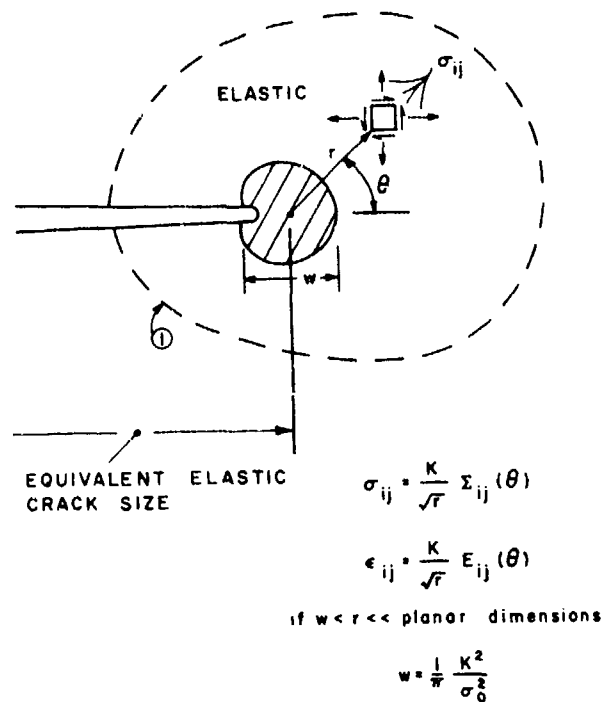
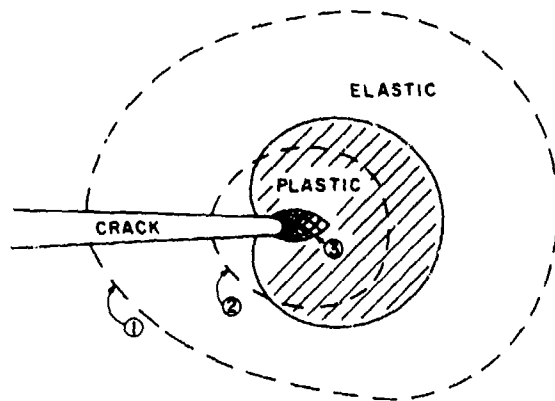


Figure 9. Linear-Elastic Crack-Tip Stress and Strain Fields (Reference 13).

2.1.2 Elastic-Plastic Field Parameters

The solutions for the in-plane tensile opening mode (Mode I type) of deformation problems are the primary interest in the present work as well as fracture mechanics in general. However, the mathematical difficulties have prevented detailed treatment of elastic-plastic problems. Except in some out-of-plane, tearing mode (Mode III type) of problems^{16,17}, rigorous mathematical solutions of elastic-plastic problems are not available in general; the available limited cases of elastic-plastic crack tip stress analyses will be reviewed in this paragraph.

Figure 10 shows the crack tip and area ahead of the crack tip¹³. The region ahead of the crack-tip is divided into three distinct zones: (1) elastic, (2) elastic-plastic, and (3) intensely nonlinear (large strains and rotations, and ductile cavities) zone. The elastic zone (1) controls the behavior when the plastic zone size is small compared to the



- Zone 1 = An Elastic Field Surrounding the Crack Tip
- Zone 2 = An Elastic-Plastic Field Surrounding the Crack Tip
- Zone 3 = An Intense Zone of Deformation

Figure 10. Crack-Tip Stress and Strain Fields Surrounding the Crack (Reference 13).

elastic boundaries. In this case, referred to as small scale yielding, LEFM is applicable. If the plastic zone size is large, compared to the case of small scale yielding, LEFM is not applicable.

The intense elastic plastic stress-strain field contained within zone 2 of Figure 10 is further expanded in Figure 11.

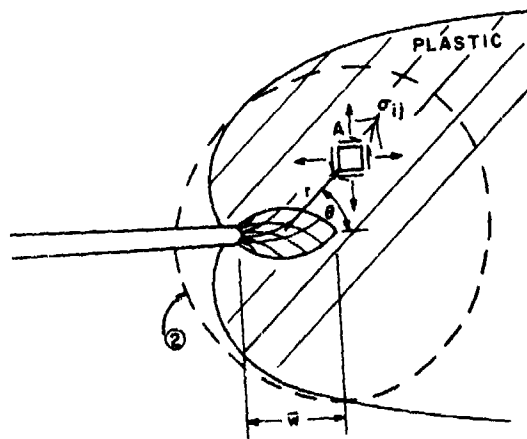


Figure 11. Expanded View of the Elastic-Plastic Stress-Strain Field (Reference 13).

When the intensely deformed process zone is small compared to the size of the elastic-plastic zone under consideration, the deformation theory of plasticity for a power hardening material can be used to obtain stress-strain solutions ahead of the crack tip outside the intensely deformed process zone as suggested by Hutchinson¹⁸ and Rice and Rosengren¹⁹. These authors expressed power hardening using a stress (σ)-strain (ϵ) relationship that is given by:

$$\sigma = \sigma_0 \left(\frac{\epsilon}{\epsilon_0} \right)^N \quad (4)$$

where σ_0 and ϵ_0 are the flow stress (yield strength) and strain, respectively, and N is the strain hardening exponent.

When Equation 4 is used to model the behavior of the material in the plastic range, the stress, strain, and displacement functions for the crack tip region are given by Equation 5, regardless of the amount of plastic deformation:

$$\sigma_{ij} = K_\sigma \cdot \tilde{\sigma}_{ij}(\theta, N) \cdot r^{-\frac{N}{N+1}} \quad (5a)$$

$$\epsilon_{ij} = K_\epsilon \cdot \tilde{\epsilon}_{ij}(\theta, N) \cdot r^{-\frac{1}{N+1}} \quad (5b)$$

$$u_i = K_\epsilon \cdot \tilde{u}_i(\theta, N) \cdot r^{\frac{1}{N+1}} \quad (5c)$$

where K_σ and K_ϵ are the magnitudes of singularities of appropriate quantities with K_ϵ being a function of K_σ . The functions $\tilde{\sigma}_{ij}$, $\tilde{\epsilon}_{ij}$ and \tilde{u}_i depend on angle and exponent N in Equation 4. Equations 5a, 5b and 5c has been referred to as the set of "HRR" field equations after the initial investigators^{18,19}.

In the derivation of the HRR field equations, the deformation theory of plasticity was used to describe the material behavior. Thus, when unloading occurs during deformation, the loading path is different from the proportional loading assumed and the validity of the above solutions is not guaranteed.

The magnitude of the singularity in Equation 5 in terms of J can be written as¹³

$$\sigma_{ij} = \sigma_0 \left(\frac{J}{r \sigma_0 \epsilon_0} \right)^{\frac{N}{N+1}} \tilde{\sigma}_{ij}(\theta, N) \quad (6a)$$

$$\epsilon_{ij} = \epsilon_0 \left(\frac{J}{r \sigma_0 \epsilon_0} \right)^{\frac{1}{N+1}} \tilde{\epsilon}_{ij}(\theta, N) \quad (6b)$$

$$u_i = \epsilon_0 \left(\frac{J}{\sigma_0 \epsilon_0} \right)^{\frac{1}{N+1}} r^{\frac{N}{N+1}} \tilde{u}_i(\theta, N) \quad (6c)$$

when the process zone is small. The J parameter is given by the contour integral²⁰

$$J = \int_{\Gamma} w dy - \vec{T} \cdot \frac{\partial \vec{u}}{\partial \vec{x}} ds \quad (7)$$

which has been determined to be independent of the location of the contour curve Γ .

Hence, for a given material, with the assumption of power law hardening behavior, deformation theory of plasticity, and proportional loading, there exists a unique elastic-plastic stress and strain field which is characterized by its intensity J. In a manner similar to the LEFM approach where K measures the intensity of stress and strain within the elastic crack tip field, the parameter J defines the intensity of the elastic-plastic stress and strain at the crack tip field and thus provides a basis for a nonlinear fracture mechanics approach. The use of J to define the level of elastic-plastic stresses and strains around the crack tip requires that the intensely deformed process zone is small.

For ideally plastic materials, the relationship between the J-Integral and the crack tip opening displacement (defined by the opening distance between the intercepts of two 45° lines, drawn back from the crack tip, with the deformed profile of the stationary crack) is given by^{20,21}.

$$J = \alpha \sigma_0 \delta_t \quad (8)$$

where α is a constant. More recently Shih and co-workers^{22,23} have shown that Equation 8 can be used to relate J and δ_t for strain hardening materials where the constant α is replaced with a function which is strongly dependent on the strain hardening exponent and mildly dependent on the ratio σ_0/E . On the basis of Equations 6 and 8, δ_t , the crack tip opening displacement, is also a parameter which characterizes the intensity of the stress-strain HRR field. The above HRR field equations are applicable only for the case of stationary cracks.

Much of the current research in modeling "High-FCGR" behavior utilizes the assumption that the HRR field equations are applicable to quasi-static moving cracks. Paris¹³ has suggested an argument to justify the J-Integral for FCGR studies based on the following logic:

For high rates of growth, the crack tip moves ahead during each cycle into relatively new material in terms of plastic deformation, compared to the intense deformation it will sustain at the crack tip during the next cycle. Thus, during the next cycle, past history will not be significant compared to the loading, which is then being sustained. As long as a moving crack is considered, it may be possible to neglect past history including unloading in a J-Integral analysis and characterization of material behavior.

Rice²⁴ suggests that a crack tip integral similar to J can be defined for cyclic loadings if the alteration $\Delta\sigma_{ij}$ of stress (i.e. the stress range) following any load maximum or minimum is related to the corresponding alteration of strain $\Delta\varepsilon_{ij}$, for those alterations actually experienced by the material, in such a way that $\int \Delta\sigma_{ij} d\Delta\varepsilon_{ij}$ is a function only of the $\Delta\varepsilon$'s and not of position in the material. To date, no publication has appeared in which the ΔJ -Integral has been calculated by applying the integral formulation presented in Equation 7 to the crack tip region for cyclic problems. Normally, the approach taken for such loadings is to use the potential energy property of the J-Integral to calculate what is termed an operational definition of the J-Integral. In a review of Dowling and Begleys' results obtained on compact type specimens, Parks²⁶ observed that objections to the operational use of the parameter ΔJ can be rationalized away if one notes the fact that stable hysteresis loops (macroscopic load/displacements) are nearly symmetrical for reversed stressing. This observation implies that most material points are seeing fully reversed (zero mean) deviatoric stressing. The stable hysteresis loop hypothesis leads to a strain energy function (W^*) approach such that $\Delta\sigma = \frac{\partial W^*}{\partial (\Delta\varepsilon)} = \Delta\sigma (\Delta\varepsilon)$ exists for all material points in the crack tip region.

2.2 CRACK TIP APPROACH

As discussed earlier, there exists an intensely deformed region at the crack tip. The deformation processes in this intensely deformed process zone are believed to control the crack growth behavior. Instead of correlating the crack growth with the parameters that define the stress field surrounding the process zone, it should be possible to correlate the crack growth with parameters identified within the process zone directly.

This section identifies currently available crack tip parameters. Table 2 presents some of these parameters which have been described in the literature.

TABLE 2
FRACTURE MECHANICS CRACK TIP PARAMETERS

<u>Crack Tip Parameters</u>	<u>Symbol</u>
Near Tip Strain	ϵ_{yy}^t
Crack Tip Opening Displacement (CTOD)	δ_t
Crack Tip Opening Angle (CTOA)	α_t
Crack Opening Angle (COA)	α_o
Crack Tip Nodal Force	F
<u>Energy-Based Parameters</u>	
Crack Separation Energy Rate	G_Δ
Change in Energy Rate in Process Zone	G_p
Generalized Energy Release Rate at the Process Zone ($G = G_\Delta + G_p$)	G

2.2.1 Crack Tip Parameters

A series of investigations have attempted to develop a cause-effect model for crack advance by correlating the level of stress-strain displacement related parameters in the crack tip region with the amount of crack extension. In this subparagraph, those investigations most relevant to the fatigue crack growth problem are considered.

2.2.1.1 Near Tip Strain Parameter

To enhance our understanding of fatigue crack growth behavior, several investigators have employed a critical strain model. The critical strain model is based on the concept that an element of material, which is one da/dN wide, will fail when the strain associated with that location in the material reaches a critical level. The various critical strain models are based on the level of accumulated plastic strain²⁶, maximum strain^{27,28}, or strain ranges associated with inducing a sufficient amount of fatigue damage in the element²⁹⁻³². The strain range modeling approach might be more properly called a fatigue damage approach because failure in the material element is hypothesized after a sufficient amount of fatigue damage has been induced by the intense cyclic action as the crack propagates toward the material element. The results of this approach have provided better correlations with FCGR damage as the analytic descriptions of the crack tip stress and strain fields have improved.

One important and particularly interesting feature of the near tip strain parameter approach is that the strain in the crack tip region can be experimentally measured^{29,33,34}, making direct correlations between this parameter and the resulting FCGR damage possible. Further, as Newman²⁹ has shown, a maximum strain criterion can be used as a simple criterion for crack advance in a cyclic finite element program. Newman suggests that when the maximum strain in the crack tip element reaches a critical level the crack tip node is released and the crack advances to the next node in line. Using this approach, Newman has been able

to successfully reproduce the experimentally observed crack opening and closing stress results of Elber³⁵.

2.2.1.2 Crack Tip Opening Displacements and Angles

The near-tip field in crack-growth situations is different than in the stationary case. There is no complete description of the stress and strain fields ahead of a extending crack. Some insight has emerged due to work by Rice³⁶, Chitale and McClintock³⁷ and Amazigo and Hutchinson³⁸. These studies revealed a milder strain singularity of the form $\ln(1/r)$ for elastic-plastic materials. The studies by Rice³⁶ based on J_2 flow theory of plasticity for an ideally plastic material showed that the incremental strains at the crack tip point are related to an increase of the crack opening displacement $d\delta$, and the increment of the crack extension da . Hence, the strains at the crack tip are uniquely characterized by the crack opening angle, $d\delta/da$.

The crack tip opening displacement (δ_t) and crack tip opening angle (α_t) parameters have been used by Shih et al.³⁹ and Kanninen et al.⁴⁰ to predict the initiation and stable growth of cracks subjected to monotonic loading. The real interest in these parameters is created by the potential for quantifying the level of crack opening either from experimental measurements or by numerical analysis. The concept of using δ_t and α_t as FCGR correlation parameters is attractive since, for each subcritical crack advance (da/dN) that occurs during the application of a cyclic load, the crack will only open a finite amount. One of the major difficulties that restricts the utility of these parameters is the lack of agreement on where the measurements should be made.

Figure 12 provides a schematic which describes the locations where measurements should be taken for comparison to available analytical results. Two definitions of the crack opening displacement and crack opening angle have been used in the literature. Crack opening displacement (δ_t) can be measured either at the original crack tip (δ_o) or at a fixed

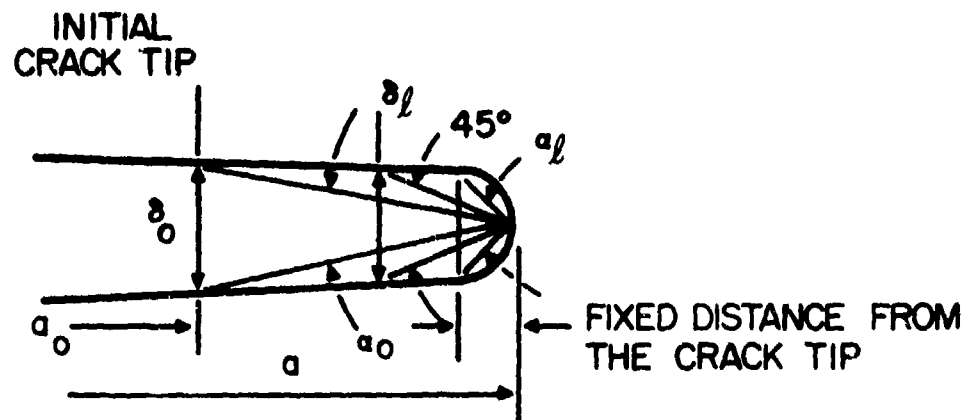


Figure 12. Crack Tip Displacement Related Parameters. Two Definitions of Crack Opening Angle and Displacement.

angle (45°) from the crack tip (δ_ℓ). The two possibilities of the crack opening angle are that it is measured either at the original crack tip (α_0) or at a fixed distance away from the crack tip (α_ℓ).

For stable crack growth, the crack opening angle stays constant as is observed by Shih et al.³⁹ and Kanninen et al.⁴⁰ in their numerical simulation and experimental measurements of α . Therefore, there exists a theoretical, numerical and experimental basis for the use of a crack opening angle as a crack growth criterion. Also, the crack tip opening angle can be measured experimentally, though such measurements may be difficult at high temperatures.

One of the disadvantages of this method is the lack of a unique definition for crack opening angle or displacement. Crack-tip opening angles and or displacements are defined in the literature at a fixed distance behind the crack-tip or at the original crack tip. The theoretical basis for using crack tip displacement parameters which characterize the crack growth is derived only for the case of monotonically increasing load, but this solution is shown to be valid experimentally and numerically for small elastic unloading occurring due to crack growth in the process zone. Although the requirement exists for more sophisticated solutions for a growing crack under fatigue conditions, investigators^{39,40} suggest that the crack opening angle may correlate the FCGR behavior generated under elastic-plastic conditions.

Finite element computational procedures have shown that the COA is not appreciably sensitive to the mesh size. Further work is necessary in this area to see whether this parameter is applicable for FCG situations.

2.2.1.3 Crack-Tip Node Force (F)

Kanninen et al.⁴⁰ have proposed that at a constant critical force at the crack-tip node, crack growth occurs. They have shown that this critical node force criterion performs well in the case of stable crack growth situations under elastic-plastic conditions.

The main disadvantage of this method is that this critical force is sensitive to the finite-element mesh and the increment step, although it stays constant during stable crack growth for a particular mesh.

Crack tip node force (F) can be evaluated from a numerical simulation of the crack growth. Hence, this parameter could be extended for fatigue crack growth situations.

2.2.2 Energy-Based Parameters

The generalization of Griffith's energy balance concept to account for nonlinear material behavior has been addressed by many investigators in an attempt to define crack growth parameters (especially stable crack growth parameters). An early continuum approach to generalizing the Griffith energy balance is given by Rice⁴¹ under the assumption of small geometry changes. The resulting energy balance takes the form of

$$G-P = 2\gamma \quad (9)$$

where G is the energy release rate, P is the plastic work rate, and the surface energy γ is interpreted as the work per unit area required to create new surfaces. For materials in which the stress saturates to a finite value at large strain, Rice⁴¹ showed that there is no energy surplus from the continuum calculation which can be equated to the work of separation. At the other extreme, when the material is elastic, the plastic work rate term is zero. Therefore, the difference G-P varies from G to zero, when the hardening behavior of material varies from elastic to perfect plastic.

Kfouri and Miller^{42,43} have presented finite element solutions for the crack separation energy rate (G_{Δ}) which is related to the work done in separating the crack. The crack separation energy rate (G_{Δ}) is obtained by quasi-static unloading of a finite element of width Δa at the crack tip, while the applied stress is maintained constant on the structure. Through analyses of the relations between G_{Δ} and Δa , a fracture criterion can be suggested by taking Δa and G_{Δ} as characteristic of the material. The results indicate that a criterion of this kind predicts stable crack growth when the step size is small compared to the yield zone, at least under small scale yielding conditions. The results also show that unstable fracture occurs immediately when the step size is greater than the maximum radius of the plastic zone^{42,43}.

Kanninen et al.⁴⁰ have also proposed that a process zone energy release rate (G_p), i.e. the change in energy contained in the process zone, will correlate with stable crack growth behavior in elastic-plastic fracture. The crack tip process zone is the region at the crack tip where non-proportional loading occurs during crack growth. Some believe that the energy flow to this process zone is a measure of the strains and stresses at the extreme tip of the crack and hence can be used to correlate the fracture process occurring at the crack tip.

The size of the process zone used for computing the energy change of this zone due to the growth of the crack is dependent on the interpretation of the investigators who have studied this approach. Kanninen et al.⁴⁰ define the size of the process zone as equal to the plate thickness for their calculations, whereas Shih et al.³⁹ define its size as five times the crack tip opening displacement ($5\delta_t$). Green and Knott⁴⁴ define a process zone by considering the spacing of inclusions and ductile fracture by cavities. In their process zone, strains are large and approximately equal to the fracture strain. For materials with a low work hardening rate, they find that the size of the process zone is twice the crack-tip opening size; for a high work hardening rate, the

material's process zone size is less than twice the crack tip opening displacement. Hence, the size of the process zone appears to be a material parameter which depends on inclusion spacing.

During stable crack growth, G_p remains constant, so G_p may be a reasonable parameter to characterize the crack growth. Energy criteria are evaluated numerically and the major disadvantage of this parameter is that it is sensitive to the mesh size.

A generalized energy release rate (G) is defined as⁴⁰

$$G = G_p + G_{\Delta} \quad (10)$$

which is equal to the energy flow across the boundaries of the process zone during the elastic-plastic stable crack growth (See Figure 13). For stable crack growth, this value of G seems to remain constant. The computed value of G is insensitive to the finite element mesh size and thus this parameter may provide a reasonable criterion for studying elastic-plastic fatigue crack growth behavior.

2.3 EVALUATION OF EPFM PARAMETERS

In order to correlate high fatigue crack growth rates using EPFM parameters, it is necessary to have the capability to calculate these parameters. The results of continuum analyses of elastic-plastic crack tip material behavior are limited to idealized geometries, material behavior, and loading conditions. Even in those limiting cases, a complete quantification of the behavior by analytical methods is practically impossible. Among a number of approximate numerical analysis techniques, the finite element analysis provides the best approach to this task. In this paragraph, some important considerations associated with applying the finite element method for crack tip analysis are reviewed. The results presented in this section deal with monotonic loading conditions since cyclic crack tip analysis is still in a state of infancy. We expect that cyclic loading will further complicate

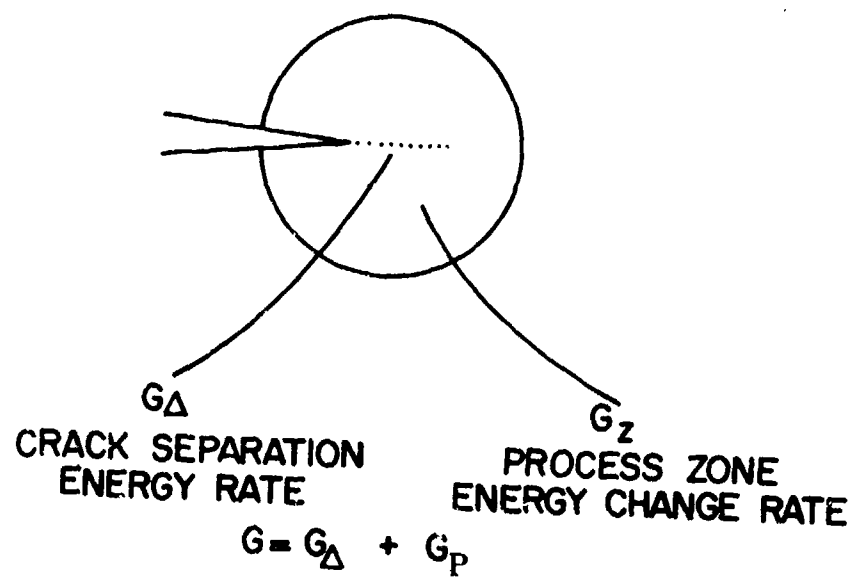


Figure 13. Generalized Energy Release Rate (G).

finite element analysis of the crack tip beyond that which is illustrated for monotonic loading.

2.3.1 Crack Tip Analysis by Finite Elements

In the modeling of an elastic-plastic continuum which contains a crack, two features of the crack geometry must be given special consideration: (1) the crack tip singularity, and (2) the extent of crack tip shape changes (blunting). In the paragraphs below, we will outline several finite element modeling approaches which deal with these geometric features.

2.3.1.1 Crack Tip Singularity Modeling

For problems with singularities, Tong and Pian⁴⁵ have shown that the convergence rates of the finite element solutions are dominated by the nature of singularity near the crack tip. Unless these singularities are properly represented in the assumed solution functions, even with regular so-called high-accuracy elements (with higher order polynomials as interpolates), the rate of convergence of solutions cannot be improved. However, when the functions for the singularity are incorporated explicitly in the assumed solution in the near crack tip elements, in general the satisfaction of the convergence criteria for the finite element solution⁴⁶ is not guaranteed. Current finite element approaches for solving crack tip problems fall into two general classes.

The first approach ignores the singular nature of the solution (Equation 5) in those finite elements near the crack tip and uses regular assumed solution functions⁴⁷⁻⁵⁰. This approach ensures that the finite element convergence criteria are satisfied but requires a very fine finite element grid near the crack tip to obtain reasonable results at or close to the crack tip. A disadvantage of this approach is that it is costly.

The second approach incorporates appropriate functions for the singularity in the crack tip elements⁵¹⁻⁵⁹ in one of the following ways:

(a) Exact crack tip singularities are included in the near crack tip elements. In this way, the singular solution can be represented accurately with relatively few elements, but the compatibility of displacements between crack tip and regular elements is not assured.

(b) Crack tip elements are represented by degenerated isoparametric elements or quarter point 8-noded isoparametric quadrilateral elements. This approach requires no special coding for elements at the crack tip, introduces no incompatibility, and involves no extra cost.

(c) The third approach utilizes a hybrid finite element⁵⁴⁻⁵⁷ in the modeling. The solution functions in these crack tip elements are chosen so that the singularity is appropriately modeled. The interelement continuity condition, which is required as a convergence criterion, is not violated due to the presence of the singular functions. The interelement continuity condition is enforced as an a posteriori condition of extremization of the modified energy function by a Lagrange multiplier method.

Table 3 summarizes the advantages and disadvantages of the two general classes of finite element approaches.

2.3.1.2 Crack Tip Blunting

The other problem involved in the finite element formulation for elastic-plastic crack analyses is the development of a finite element grid which will model the configuration of the crack tip blunting during loading. Large deformation analysis is required in the investigation of the crack tip blunting. McMeeking⁵⁸ studied the crack tip finite deformation configuration for small scale yielding by using the very fine mesh of 4-node quadrilateral isoparametric finite elements shown in Figure 14. After a sufficient amount of load was applied, he expected that the steady-state solution for contained yielding to be largely independent of original geometry of the crack tip. When the crack tip opening was more than double the original opening, the

TABLE 3
COMPARISON BETWEEN FINITE ELEMENT MODELS FOR FRACTURE ANALYSIS

MODEL	FEATURES	ADVANTAGES	DRAWBACKS
I. Conventional Refined Elements at the Crack Tip	<ul style="list-style-type: none"> • Does Not Include Crack Tip Singularity Explicitly • Satisfies Convergence Criteria (Compatibility) 	<ul style="list-style-type: none"> • Simplicity in Formulation • Easy to Apply With General Purpose Programs 	<ul style="list-style-type: none"> • Expensive • Inefficient
IIa. Conventional Element with Embedded Singularity	<ul style="list-style-type: none"> • Incorporates Crack Tip Singularity 	<ul style="list-style-type: none"> • Simple in Formulation 	<ul style="list-style-type: none"> • Compatibility of Special Elements With Host Elements Are Not Guaranteed
IIb. Conventional 8-noded Isoparametric Quadrilateral Element With Degenerate Quarter Point Elements at the Crack Tip	<ul style="list-style-type: none"> • Incorporates Crack Tip Singularity • Satisfies Convergence Criteria 	<ul style="list-style-type: none"> • Easy to Apply With General Purpose Programs • Blunting Can Be Considered • Inexpensive 	<ul style="list-style-type: none"> • Rectangular Element Have a Singular Stiffness at the Crack Tip
IIc. Hybrid Formulation	<ul style="list-style-type: none"> • Incorporates Crack Tip Singularity • Satisfies Convergence Criteria 	<ul style="list-style-type: none"> • Efficient • Fast Convergence Rate 	<ul style="list-style-type: none"> • Complicated Formulation

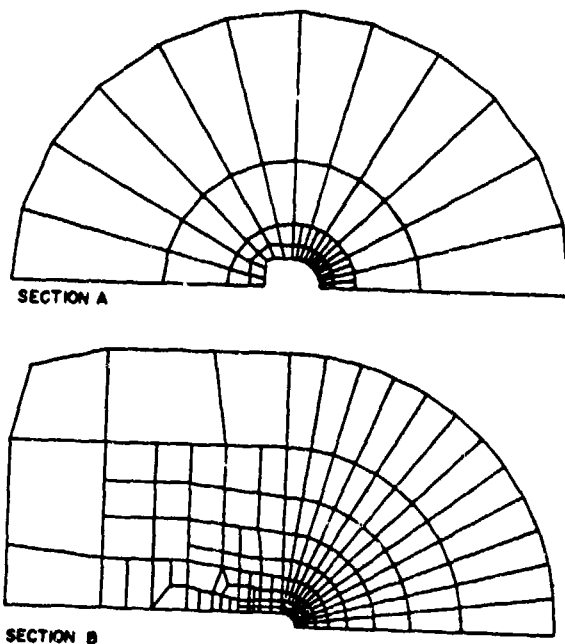


Figure 14. Undeformed Configuration of Finite Element Mesh for the Notch-Blunting Solution (Reference 58).

solutions for continuing load increments settled down to a steady level in which increments of all quantities with length dimensions (such as crack tip opening and plastic zone size) are scaled with increments of J/σ_0 . McMeeking computed the J parameter on contours remote from the tip. Thus, above a certain load level, McMeeking's finite element grid appears to represent, with reasonable accuracy, the blunting behavior of the initially sharp crack tip.

Shih et al.³⁹ utilized degenerate 8-node isoparametric quadrilateral elements as discussed by Barsoum⁵⁹ for the singular crack tip element as shown in Figure 15. In the figure, only the corner nodes are indicated. The crack tip elements with triangular shape in Figure 15a are 8-node quadrilateral elements in which the two corner nodes and the corresponding mid-side node are initially collapsed to a common point at the crack tip. As the load is increased, the crack tip blunting is modeled by separating the nodes at the common points, as shown in Figure 15b.

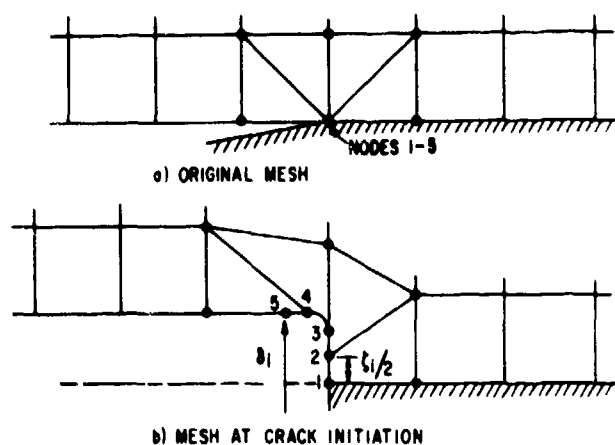


Figure 15. Finite Element Mesh for Crack-Tip Blunting
(Reference 39).

2.3.2 Numerical Estimation of the J-Integral

Shih et al.²² have proposed a procedure to estimate crack tip parameters J and δ_t which were generated for several cracked structures manufactured from materials that can be modeled using

$$\frac{\epsilon}{\epsilon_0} = \left(\frac{\sigma}{\sigma_0} \right) + \alpha \left(\frac{\sigma}{\sigma_0} \right)^n \quad (11)$$

The structures considered were center-cracked, single-edge-notched, compact tension and three point bend specimen geometries. The Shih, et al. procedure is based on a series of solutions to boundary valued problems where only the strain hardening part, $\alpha(\sigma/\sigma_0)^n$, of Equation 11 is used to model the material. They have observed that when the solutions involve a monotonically increasing single load parameter, P , all stress and displacement parameters increase in direct proportion to the load parameter raised to a power dependent on the strain hardening exponent, n . The value of J obtained for a center-cracked panel made from a strain hardening material is given by:

$$J = \alpha \sigma_0 \epsilon_0 a \left(\frac{b-a}{b} \right) \cdot g_1 \left(\frac{a}{b}, n \right) \cdot \left(\frac{P}{P_0} \right)^{n+1} \quad (12)$$

where a is the half crack length, b is the half width of the specimen, g_1 is a function of $\frac{a}{b}$ and n . Equation (12) will provide a simple functional relationship which can be used to compute J for different load levels. These simple functional relationships of J or δ_t for different geometrical configurations would provide a simple method of evaluating these parameters for different crack lengths and materials (different values of a and n).

Once the solutions given by Equation 12 are established, these can be employed together with linear elastic solutions to produce approximate formulas for the estimation of J and crack opening displacement which are valid in the transition region between small-scale yielding and large-scale yielding.

2.3.2 Concluding Remarks on Finite Element Results

Numerous reports on the finite element analyses of elastic-plastic fracture problems are presently available. The potential of the finite element method as a tool to obtain quantitative solutions of practical problems with complicated geometries, and to verify approximate continuum analysis results numerically, is considerable.

The repeatability of the finite element solutions for the linear elastic fracture analysis using different analytical techniques is quite good. However, for elastic-plastic fracture analysis, different finite element methods do not always provide accurate and unambiguous solutions.

This fact is evident from the work of Wilson and Osias⁶⁰ which describes the results of a ASTM round-robin investigation which was conducted (around 1973-1974) to compare the results of ten different state-of-the-art finite element solutions of a cracked three-point bend specimen. As can be seen from Figure 16, the discrepancies between the various analyses at high load levels are significant.

The letters on each curve of Figure 16 represent the analyses described in Table 4. Unfortunately, no experimental results are available for comparison. ASTM Subcommittee E24.08 on Elastic Plastic Fracture is currently involved in a new round-robin investigation of Finite Element Computational Capability.

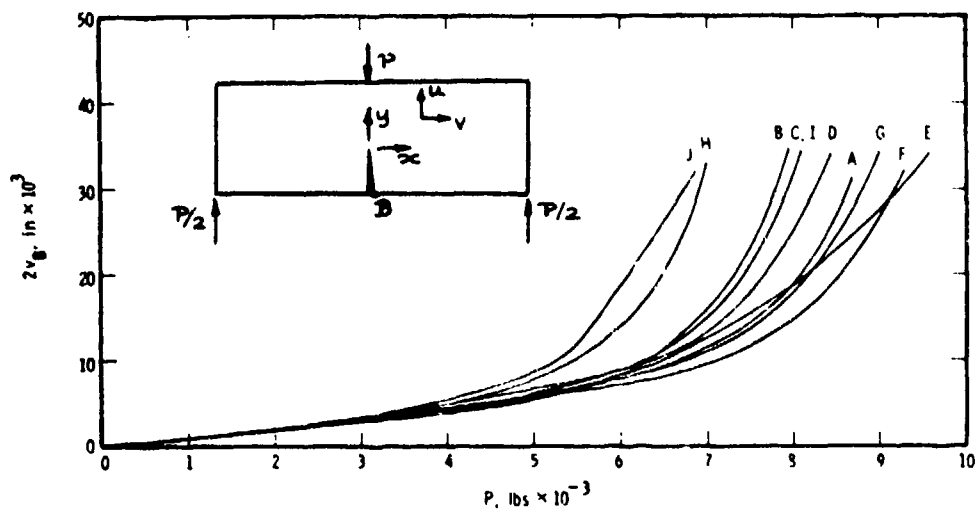


Figure 16. Crack Mouth Opening Displacements as a Function of Magnitude of Applied Load (Reference 60).

TABLE 4

INFORMATION OF DIFFERENT TYPES OF
FINITE ELEMENT FORMULATION (REF.59)

Solution	Finite Element Formulation Type	Plasticity Method	Element Type (Near Field)	Element Type (Far Field)
A	I	Secant Modulus (Incremental Theory)	Constant Strain Triangle	Constant Strain Triangle
B	I	Secant Modulus (Incremental Theory)	Constant Strain Triangle	Constant Strain Triangle
C	I	Initial Strain (Incremental Theory)	Constant Strain Triangle	Constant Strain Triangle
D	I	Initial Stress (Incremental Theory)	Constant Strain Triangle	Constant Strain Triangle
E	I	Secant Modulus (Deformation Theory)	6 Node Isoparametric Triangle	8 Node Isoparametric Quadrilateral
F	I	Initial Strain (Incremental Theory)	8 Node Isoparametric Quadrilateral	8 Node Isoparametric Quadrilateral & 6 Node Triangle
G	II	Quasi-Linearization and Iteration (Deformation Theory)	Singular Crack Tip Element (1 Circular Element)	12 Node Isoparametric Quadrilateral
H	II (Hybrid)	Initial Stress (Incremental Theory) Kinematic Hardening	Singular Crack Tip Elements (5 Triangles)	8 Node Isoparametric Quadrilateral
I	II	Tangent Modulus (Incremental Theory)	Singular Crack Tip Elements (8 Triangles)	9 Node Bi-Quadratic Isoparametric Elements
J	II	Tangent Modulus (Incremental Theory)	Singular Crack Tip Elements (3 Triangles)	8 Node Isoparametric Quadrilateral

SECTION III
SUMMARY OF AVAILABLE DATA

In this section of the report, FCGR data are identified that have been collected under conditions which induce extensive crack tip yielding. The section is organized so that attempts to correlate FCGR data with LEFM parameters are presented first. These correlations are followed with a summary of currently available J-Integral work. Finally, all other known correlations of FCGR data with other parameters are summarized.

3.1 THE FCGR LEFM PARAMETER CORRELATIONS

3.1.1 Stress Intensity Factor Correlations

As indicated in Section 1, Frost et al.⁴, Dubensky⁵, and Dowling and Walker⁶ developed FCGR correlations based on the LEFM parameter ΔK . Each investigator found that some ductile materials in the high FCGR regime do not exhibit a correlation that is independent of the maximum applied stress. Dubensky attempted to correct for the effect of plasticity by modifying the stress intensity factor calculation through the use of an effective crack length. Dubensky's effective crack length was obtained by extending the observed crack length values by a calculated plastic zone size.

The 2024-T3 aluminum data which exhibited the maximum stress influence identified in Figure 4, still showed the stress level influence even with Irwin, Dugdale and Newman type plasticity modifications considered. Dubenski's data provide a valuable base for calculations and the details of his test program are summarized in Table 5.

In Dubensky's test program, FCGR data were collected in 12 inch wide center-cracked panels of 0.090 inch thickness for high net section stress conditions. Initial starting half-crack length sizes were in the vicinity of 0.080 inch for all tests. Described in the Table 5 is a summary of the initial and failure net section stress conditions for the FCG tests conducted on the two materials. Also provided are fracture toughness calculations.

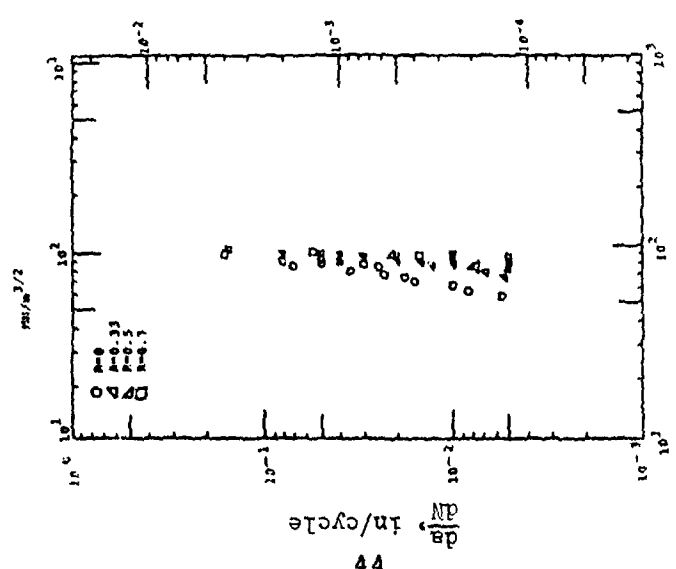
TABLE 5*
SUMMARY OF DUBENSKY'S TEST RESULTS

Material	Stress Ratios Considered	$\frac{\sigma_{net}}{\sigma_{ys}} a=0.08 \text{ inch}$	$\frac{\sigma_{net}}{\sigma_{ys}} a=a_f$ (Average)	Average a_f (inch)	Average K_{IC} Ksi/in.
7076-T6 ↓	0	0.74	0.77	0.345	57.3
	0,0.33,0.5,0.7	0.80	0.833	0.258	53.8
	0,0.33,0.5,0.7	0.87	0.985	0.199	51.3
	0,0.33,0.5,0.7	0.94	0.953	0.149	47.8
	0,0.33,0.5	0.97	0.976	0.113	45.5
2024-T3 ↓	0,0.33,0.5,0.7	0.59	1.18	3.02	110.
	0,0.33,0.5,0.7	0.79	1.08	1.67	96.2
	0,0.33,0.5,0.7	0.99	1.06	0.460	60.6
	0,0.33,0.5,0.7	1.04	1.06	0.196	41.1

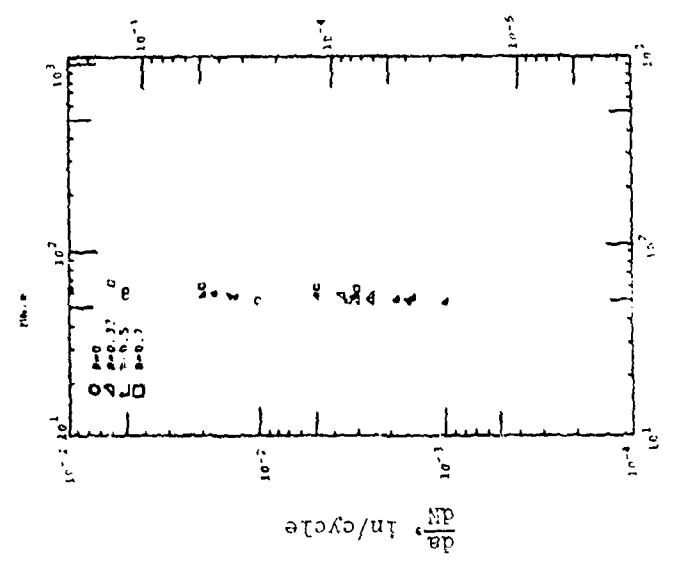
*1 in = 25.4 mm; $1 \text{ Ksi}\sqrt{\text{in}} = 1.1 \text{ MN/m}^3$

As can be noted, net section stresses at failure are above 75 percent of the yield strength for the 7075 alloy and above 105 percent for the 2024 alloy. Fracture toughness is noted to vary with the fracture half-crack length (a_f) for both materials but more dramatically for the 2024 alloy. The crack length versus cycles data, on which the FCGR data were generated, are contained in the report. The 2024-T3 aluminum alloy data for the three highest maximum stress conditions are presented in Figure X1 as a function of K_{max} . As can be seen from the Figure, the normal stress ratio (R) effect disappears as the maximum stress and crack growth rate increase. For the two highest maximum stress conditions, the FCGR cluster about a single trend line which is a characteristic for that maximum stress condition. Figure 17

$$S_{\max} = 40 \text{ Ksi} = \frac{0.78}{Kn} \frac{S_{\max}}{0.0}$$



$$S_{\max} = 50 \text{ Ksi} = 0.98 \frac{S_{\max}}{0.0}$$



$$S_{\max} = 52.5 \text{ Ksi} = 1.03 \frac{S_{\max}}{0.0}$$

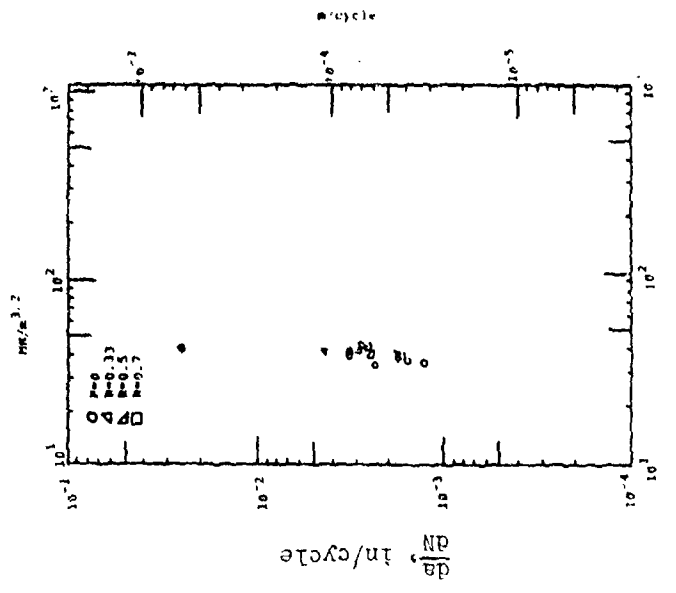


Figure 17. Dubensky's 2024-T3 FCGR Data Presented as a Function of K_{\max} for the Three Highest Levels of Maximum Gross Stress.

provides direct evidence that it may be necessary to describe FCGR above a given level using a two parameter approach where one parameter is a fracture and the other is a strength-related parameter.

Wilhem and Ratwani have been actively conducting fracture resistance testing for the last several years^{61,64}. Recently they attempted⁶⁵ to correlate the FCGR data collected by Dubensky⁵ on 2024-T3 aluminum with some of their monotonic-loading, fracture-resistance-curve test results. Figure 18 shows that they have had reasonable success in correlating the tearing crack movement (Δa) under monotonic loading conditions with the average crack advance per cycle ($\Delta a = da/dN$) for fatigue loading conditions. For both types of loadings, the maximum stress intensity factor ($K_{max} = K_R$) was used to portray the results. While Wilhem and Ratwani's results appear to be at variance with the data presented in Figure 17, it must be pointed out that Wilhem and Ratwani used Dubensky's lower maximum (gross) stress level FCGR data which appear to correlate reasonable well using LEFM correlations (See Figure 4).

Because of somewhat striking differences between the FCGR behavior generated under low and high gross stress conditions, one might first attempt a correlation on the basis of net section stress levels. As can be noted from the Table summarizing Dubensky's data, such an approach does not appear too promising. For purposes of establishing some criterion that will describe the boundary between when FCGR-LEFM correlations can or can not be used Frost et al.⁴ and Dowling⁶⁶ suggested zone criteria. The Frost et al.⁴ criterion (from Equation 2):

$$r_y = \frac{1}{2\pi} \left(\frac{K_{max}}{\sigma_0} \right)^2 \leq \frac{a}{7} \quad (13)$$

for the limiting plastic zone size is suggested as an upper bound for restricting the utility of the LEFM parameters. For the most part, Dubensky's high FCGR data generated for the lower (gross) stress maximum levels in the 2024-T3 aluminum exhibit higher (r_y/a) levels than suggested by Equation 13; conversely, the FCGR

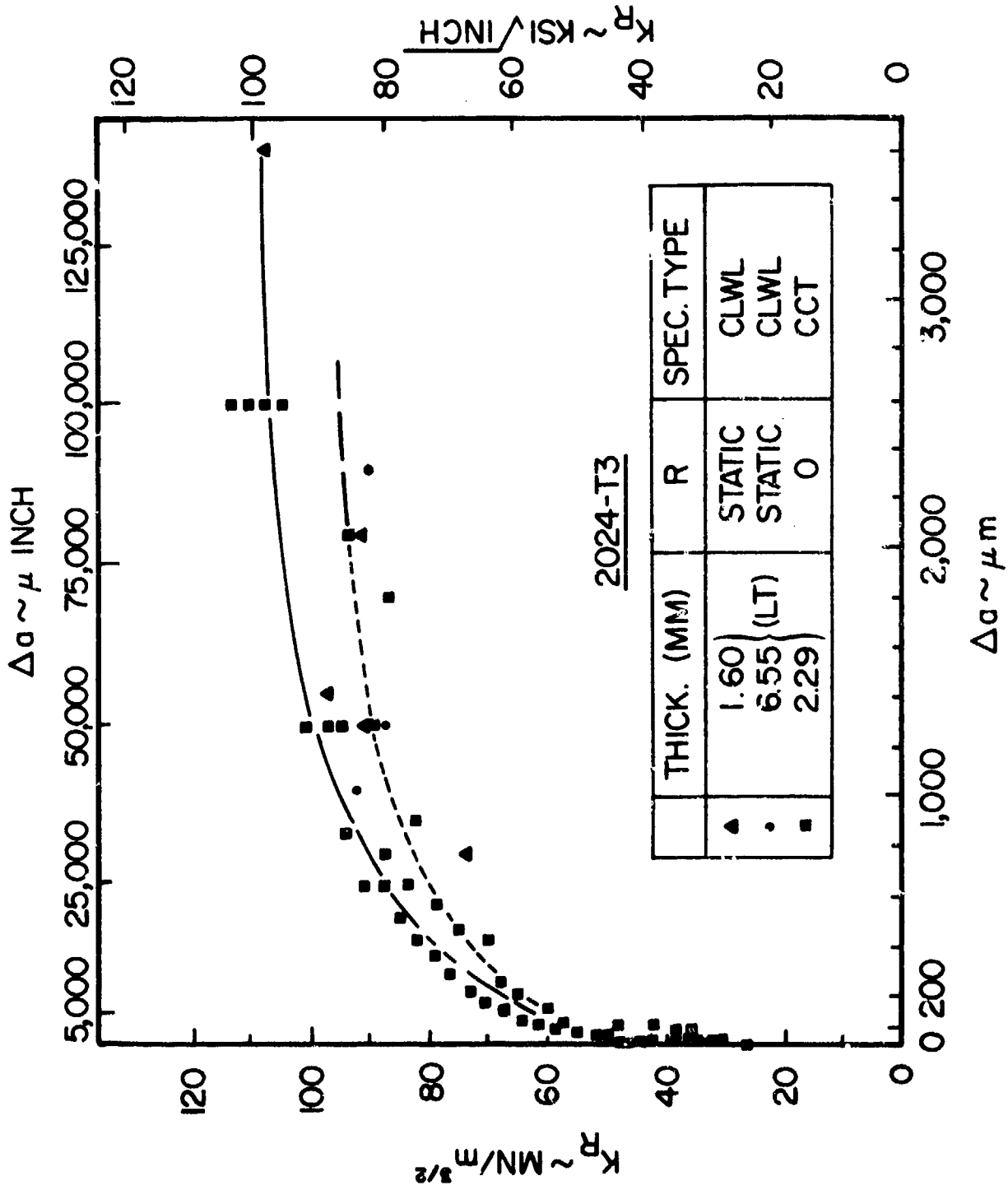


Figure 18. Correlation of "High" FCGR and Monotonic Tearing Behavior with LFM Parameter K_{max} ($=K_R$).

data generated for the higher maximum stress levels exhibit levels of the (r_y/a) parameter more nearly in line with the Frost et al.⁴ criterion.

Dowling⁶⁶ more recently considered the problem where geometric dimensions as a whole must be considered in estimating the upper limits of LEFM applicability. In this study, compact specimens were used and the specific focus was on the ratio of plastic zone size to remaining ligament, width minus crack length $(W-a)$. Dowling showed that an appropriate criterion which restricted unbounded plasticity is given by

$$r_y = \frac{1}{2\pi} \left(\frac{K_{\max}}{\sigma_0} \right)^2 < \frac{W-a}{4} \quad (14)$$

He subsequently employed this criterion to identify FCGR data, generated for Man Ten Steel, which could not be correlated utilizing the ΔK (LEFM) parameter⁶ (See Figure 5).

3.1.2 Strain Intensity Factor

In 1963, McEvily and Boettner⁶⁷ reported that they were able to describe FCGR behavior of copper between 0.002 and 0.02 mm/cycle (intermediate range) using a strain intensity range approach. More recently, Kitagawa et al.⁶⁸ have attempted to correlate the FCGR behavior associated with small micro-cracks with both a plastic strain intensity range and total strain intensity range with some degree of success using a mild steel (SB-22) in the FCGR range between 10^{-7} and 10^{-5} mm/cycle. Their studies are basically concentrated on low-range of fatigue crack growth rates, and hence the plastic zone size may have been small compared to the surrounding elastic field.

Strain intensity is a measure of the intensification of strains at the crack tip ($K_e = \epsilon \beta \sqrt{\pi a}$). The computational schemes associated with LEFM parameters which are documented in handbooks are used to find the geometrical component of the strain intensity factor where the strain is either the plastic strain range or the total strain range.

3.2 J-INTEGRAL PARAMETERS

As suggested by Equation 6, the magnitude of the stresses and strains in the elastic-plastic near crack tip stress and strain fields can be related to the value of the J-Integral, the strain hardening exponent (N), the yield strength level (σ_0) and the yield strain level (ϵ_0)^{13,18,19}. The J-Integral is a path independent line integral described by the expression presented in Equation 7. In 1968, Rice²⁰ published a paper describing the analytical properties of the parameter wherein it could be (a) correlated with the Energy Release Rate (G) for linear elastic structures, and (b) utilized with a nonlinear elastic material analysis to describe the response exhibited by elastic-plastic materials. These special properties led Begley and Landes^{69,70} to propose how this parameter could be utilized for measuring the fracture toughness of ductile materials. In particular, Begley and Landes proposed using an operational definition of the J-integral where it is assumed that the crack does not extend and that there is no material unloading within the path of the integral.

3.2.1 Operational J-Techniques - Summary

Following Dowling and Begley's²⁵ presentation at a fracture mechanics symposium in 1974, this parameter has received a great deal of attention. Dowling in subsequent work⁷¹ has been able to show that his parameter (ΔJ) correlates FCGR behavior developed from several different crack geometries (including microcrack sizes) that have been subjected to constant stress amplitude cyclic histories. Figure 19 describes the success experienced by utilizing this particular parameter. The reader will note from the figure that in the overlapping range, one can not distinguish differences between those data derived from " ΔJ " tests, where extensive plastic deformation is observed, and from tests in which the plasticity is contained under small scale yielding conditions. Others have duplicated the general observations of Dowling. In particular, Sadananda and Shahinian⁷⁴ have recently shown its application to

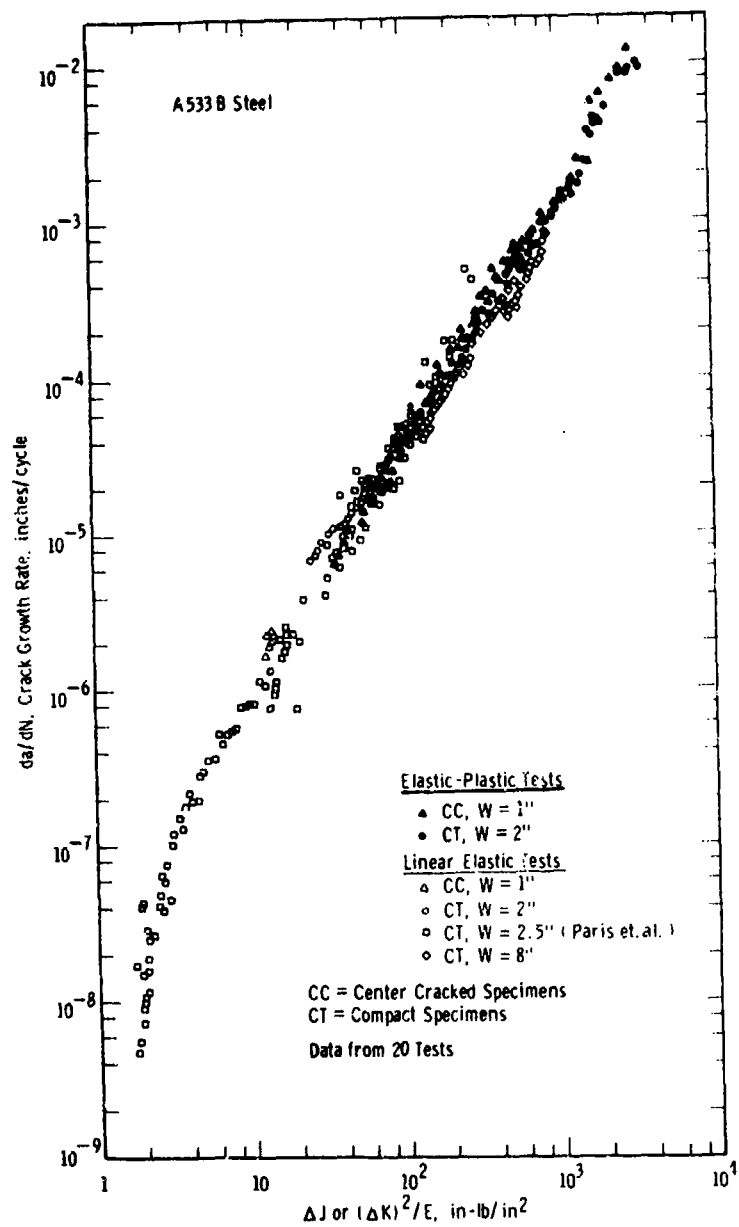


Figure 19. Fatigue Crack Growth Rate Versus Cyclic J for Various Geometries (Reference 71).

Udimet 700 at 850°C for a number of different constant stress amplitude histories.

The principal advantage of the ΔJ approach is that it appears to work and that it can be related in a quasi-sense to the plastic stress-strain field at the crack tip.

A major disadvantage of the approach is that there are several computational schemes that are currently available for actually calculating numerical values for this parameter. These calculation schemes use, as their basis, the Rivlin-Thomas⁷⁵ compliance technique applicable to calculating the energy release rate (G) for nonlinear elastic material. A schematic illustrating the essence of the compliance technique is presented in Figure 20. The difference in the area between the two load-displacement curves is equal to the energy release rate for nonlinear elastic materials. The energy release rate has been shown by Rice²⁰ to be directly equivalent to the J-Integral. While the calculation performed under monotonic loading is rather straightforward, the analyst must define a common origin for the measured cyclic load-displacement responses before starting the calculation. Two schemes have been suggested for defining the common origin for the cyclic (loading portion) load-displacement curves exhibited by compact specimens under constant amplitude loading; these are presented in Figure 21. An additional disadvantage that might also be associated with this seemingly popular technique is that to date all calculations of ΔJ have been based on experimentally derived load-displacement behavior.

From a forward looking point of view, the experimental measurement of ΔJ represents an advantage, since analytically and experimentally derived values for this parameter can be compared.

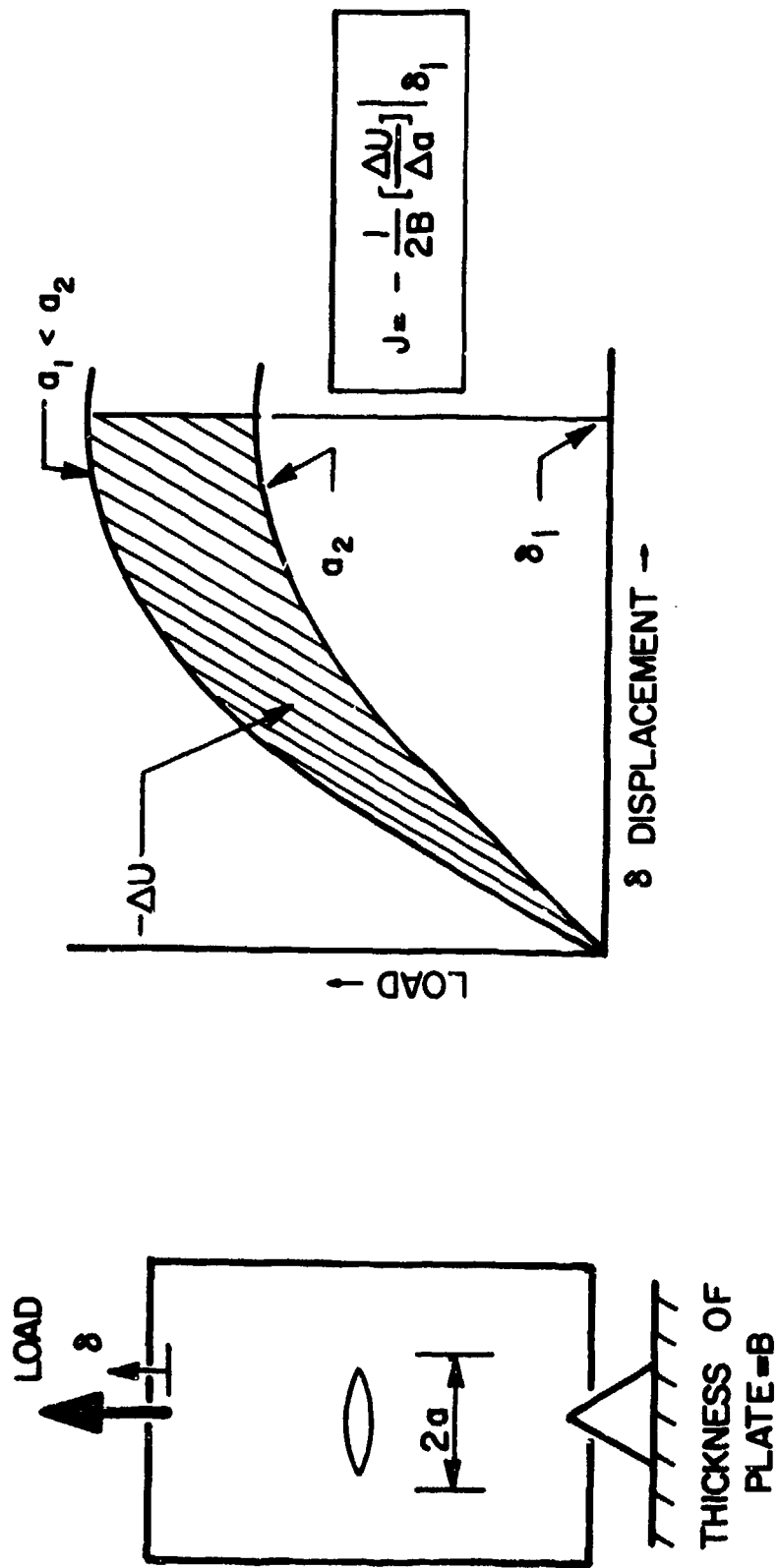


Figure 20. Procedure for Calculating Operational Values of the J-Integral.

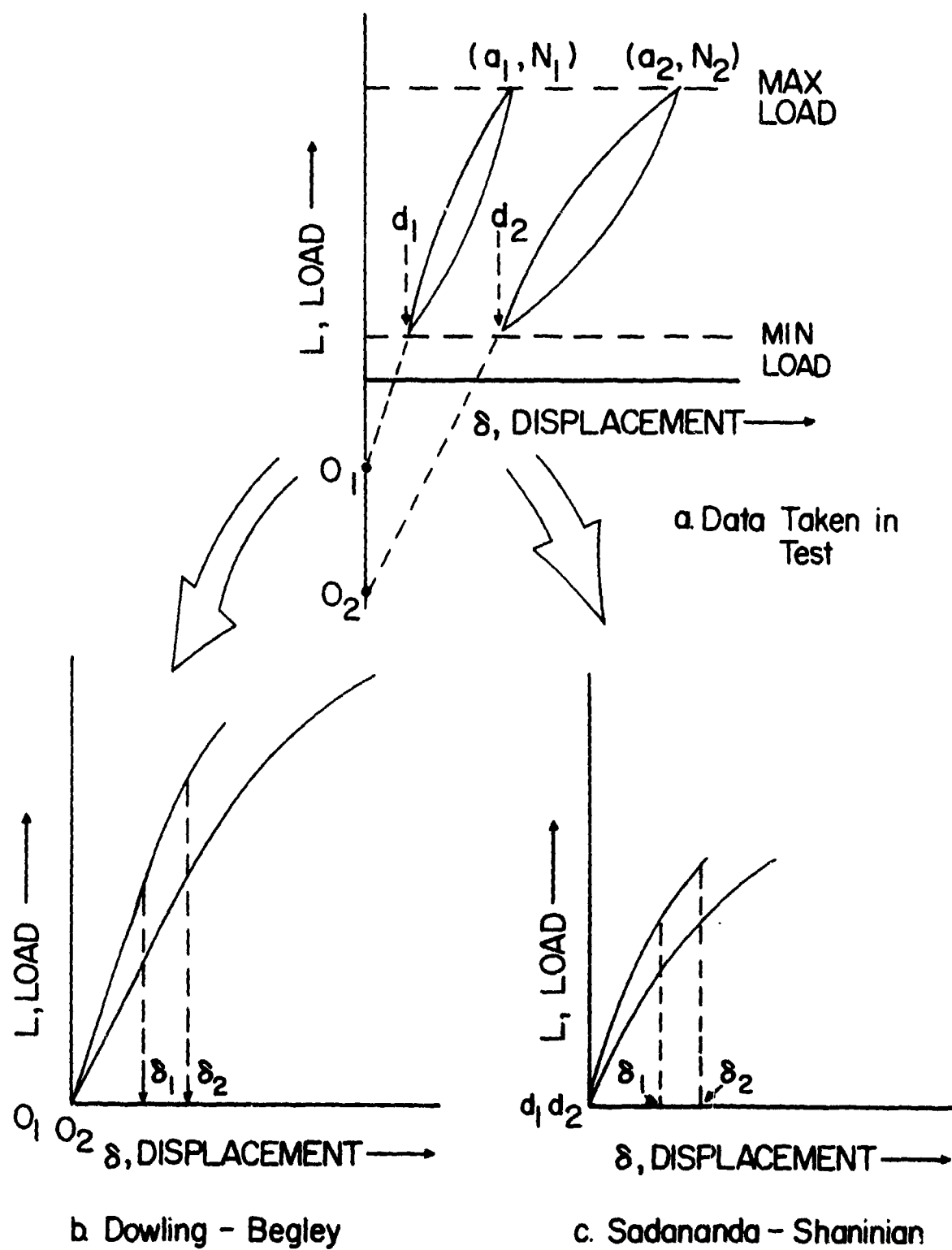


Figure 21. A Schematic Description of the Two Approaches Used to Determine Operational Values of the J-Integral - After Reference 74.

3.2.2 Operational-J Data Summary

Dowling and Begley²⁵ pioneered the use of the Operational-J approach to the FCGR correlation in the presence of gross plasticity. Compact tension fracture specimens of A533B steel were subjected to gross cyclic plastic deformations and FCGR up to 0.01 in/cycle were obtained. The FCGR data correlates with the Operational ΔJ parameter which is estimated from load versus deflection hysteresis loops. For two gross plastic specimens, ΔJ vs. N and a vs. N plots are given in this paper. For one of the above specimens, δ_{\max} (maximum deflection of the COD gauge) vs. N and crack-opening δ vs. N plots are also given. For gross plastic testing conducted under deflection control to a sloping line, FCGR correlate extremely well with the Operational ΔJ values. The tests conducted with load control to a sloping line, for large ΔJ values, FCGR deviate drastically from the straightline behavior observed in da/dN vs. ΔJ plots derived from deflection control tests. Otherwise, FCGR for both K tests and J tests is on the same power law curve.

Dowling⁷¹ continued to use the Operational-J approach to evaluate the effect of geometry on FCGR behavior. Fatigue crack growth data were obtained for center cracked specimens of A533B steel subjected to elastic-plastic cyclic loading. Cyclic J-Integral values estimated from load versus deflection hysteresis loops are correlated with these growth rate data. These results are in agreement with elastic-plastic data on CT specimens and also with linear elastic data on large size CT specimens. The tests were conducted with the load-line deflection controlled to a sloping line on load deflection planes. Hysteresis loops and crack lengths are also given for two elastic-plastic specimens by this paper.

Extension of Operational-J to the type of crack growth that occurred during low-cycle fatigue testing of smooth axially loaded specimens (LCF) fabricated from A533B Steel was investigated by Dowling⁷². Surface crack lengths were monitored periodically using cellulose acetate replicas. The estimation procedure used to obtain the Operational-J for small cracks is summarized in Figure 22. Experimental crack growth for different strain levels are correlated by Operational-J integral as shown in Figure 23. When the crack length is small ($l \leq 0.007$ in), the resulting FCGR data are found to be substantially higher than expected on the basis of available long crack-low stress type data.

When the estimation procedure for calculating ΔJ for these short cracks was modified so that crack lengths were increased by an effective crack length (l_0), El Haddad et al.⁸ have shown that the crack growth data from the small cracks in Figure 23 also can be correlated by the Operational- ΔJ parameter as shown in Figure 24. The value of l_0 is evaluated from the threshold stress intensity and the endurance limit of the material. El Haddad suggests that the microstructural features, e.g. l_0 value is a material constant that is related to the grain size for low carbon steel.

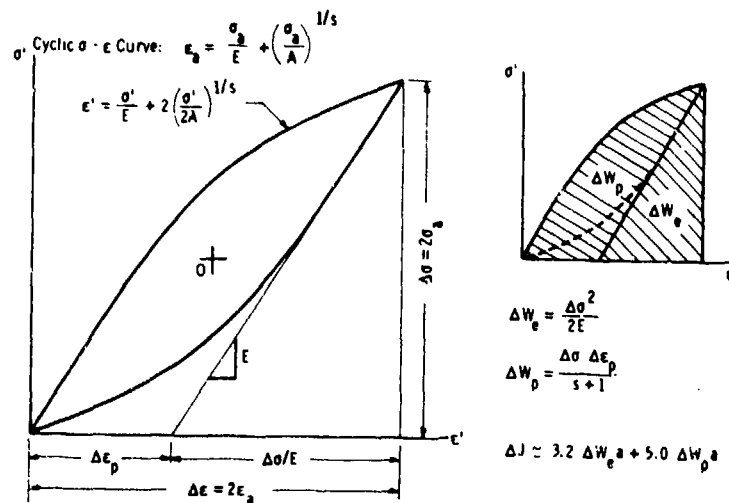


Figure 22. Estimation of Small Crack ΔJ from Stress-Strain Hysteresis Loops (Reference 72).

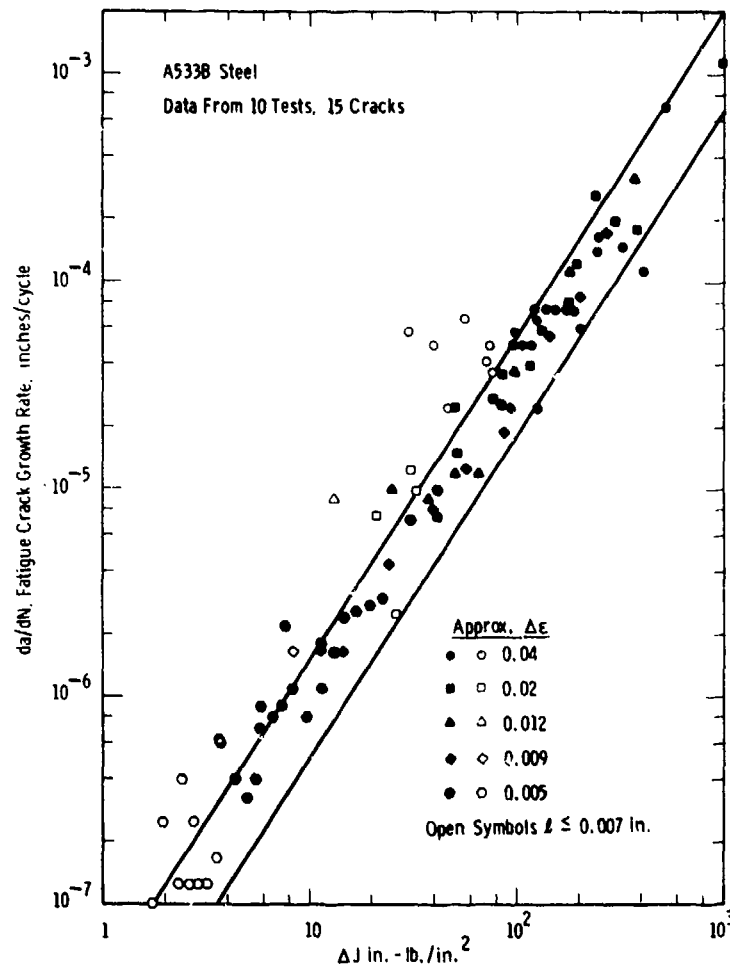


Figure 23. Comparison of Small Crack Data with Scatterband from Test Results for Ordinary and Large-Size Specimens (Reference 72).

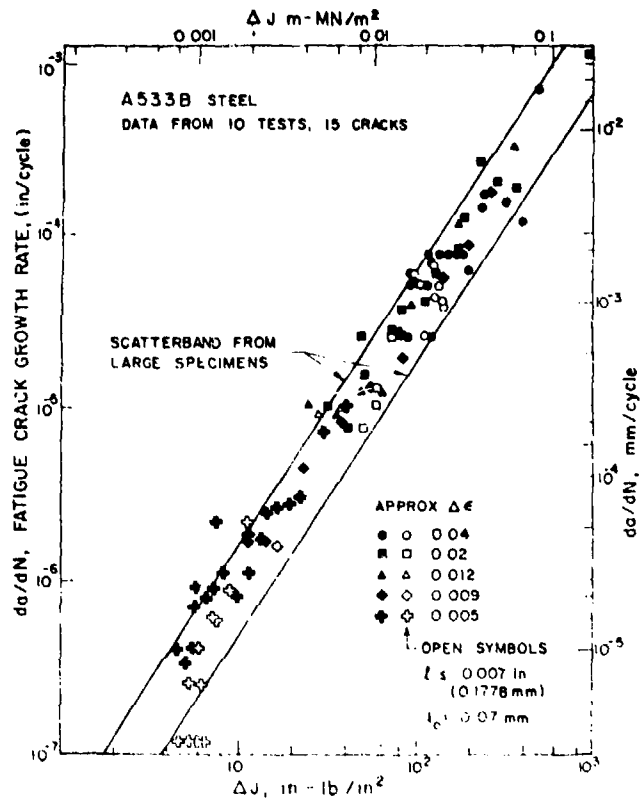


Figure 24. Fatigue Crack Growth Rates as a Function of Modified ΔJ (Reference 8).

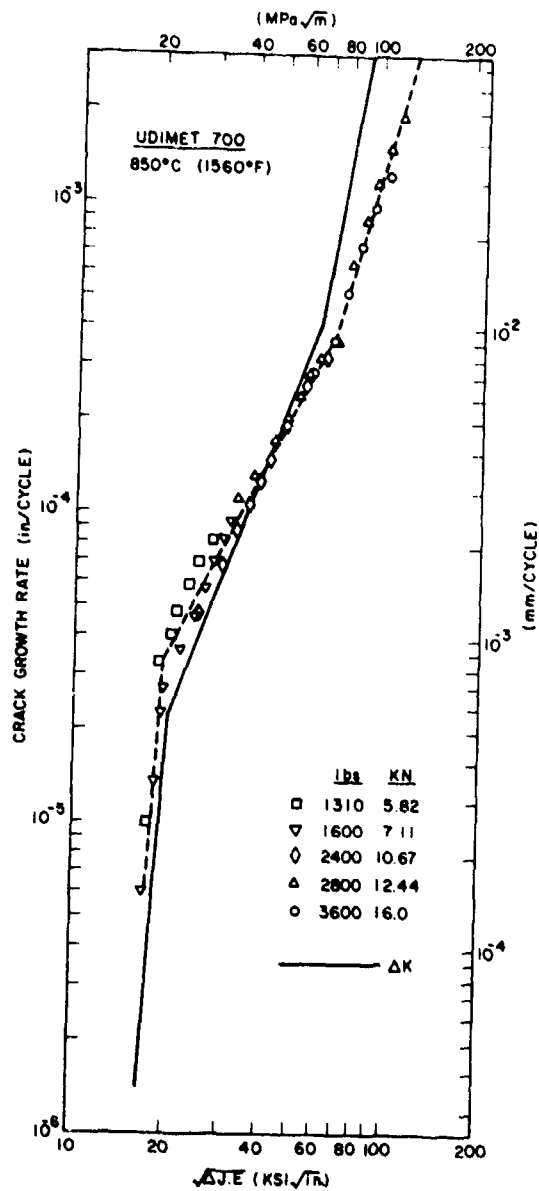


Figure 25. Crack Growth Data in Terms of ΔJ Determined Using the Merkle-Corten Approximation (Reference 74).

Sadananda and Shahinian⁷⁴ have also conducted cyclic J-Integral FCG testing on Udimet 700 at high temperature where the possibility of a larger plastic zone is likely. Fatigue crack growth rates were analyzed using both nonlinear and linear fracture mechanics where the tests were conducted at 850°C under a load control mode. Operational- ΔJ was estimated both by the compliance technique illustrated in Figure 20 and 21 and by the Rice et al.⁷⁶ estimation procedure modified by the Merkle and Corten⁷⁷ correction. One interesting feature of the Sadananda and Shahinian work is that these authors present their FCGR data in terms of an effective stress intensity factor (ΔK) calculated using the expression:

$$\Delta K \text{ (effective)} = \sqrt{\Delta J \cdot E} \quad (15)$$

In this manner, currently available FCGR data that is expressed in an LEFM format can be directly compared to new (higher FCGR) data without converting the older data to an EPFM format. Shown in Figure 25 are FCGR data that have been plotted as a function of the effective ΔK parameter calculated using the Rice-Merkle-Corten estimation procedure. The figure shows that these Udimet 700 data are described reasonably well with the trend line curve established using the more tedious compliance technique (dotted line in Figure). Furthermore, when the ΔK parameter is calculated using LEFM assumptions, the correlation with the EPFM established parameter-FCGR data values is poor.

These authors⁷⁸ have also recently shown that FCGR could be correlated by $\sqrt{\Delta J \cdot E}$ for cold worked Type 316 stainless steel at high temperatures.

Mowbray⁷⁹ studied fatigue crack growth in Cr-Mo-V steel in the high-rate regime of 2.5×10^{-4} to 2.5×10^{-1} mm/cycle with a compact type strip specimen. FCGR data were correlated as a function of ΔJ (or $\Delta K^2/E$ for elastic-plastic) for strip CT specimens both in elastic and elastic-plastic tests. Crack length versus number of cycle curves and cyclic hysteresis loops are presented for some specimens. For elastic-plastic high growth rate tests, the correlating parameter (ΔJ) is computed using the estimation procedure suggested by Bucci et al.⁸⁰.

As a consequence of specimen geometry, ΔJ apparently seems to stay constant for small ranges of crack growth. However, a careful review of Mowbray's work reveals that the specimen geometry, material, and loading combined in such a way that (a) the LEFM parameter ΔK was essentially constant with crack length, and (b) the nonlinear plastic deformation was limited. When these conclusions are reviewed collectively, the values of Mowbray's Operational ΔJ are within twenty percent of an elastic calculation ($\Delta J \approx (\Delta K)^2/E$) and therefore the test data he reports (as constant ΔJ) are really the result of a constant K control condition.

Brose and Dowling⁷³ have conducted J-Integral fatigue testing to evaluate the effect of size on the FCGR of Type 304 Stainless Steel. The da/dN versus ΔK data are compared on the basis of several size criteria which are intended to limit plasticity and hence enable linear-elastic analysis of data. The cyclic J-Integral method of testing has been employed in testing specimens undergoing gross plasticity. The data from cyclic J-Integral tests agree well with the linear-elastic tests and the results are presented using da/dN versus $\Delta K (\sqrt{\Delta J \cdot E})$ plots. Hysteresis loops are given for the specimens, which were tested using the cyclic J-Integral method of testing. Load line deflection versus crack length data are also given for the specimen which was tested under a cyclic J-Integral method of testing.

Marschall et al.⁸¹ recently generated fatigue crack growth for a cast 2-1/4 Cr-1Mo steel at an elevated temperature (540°C) under quasi- ΔJ control conditions. A typically initial loading cycle is shown in Figure 26. Loading was reversed at C and unloaded to the point E such that the maximum compressive load was equal to the prior maximum tensile load. The point D is an indication of the beginning of the crack closure. The cyclic crack growth tests were conducted with a maximum compressive load hold which corresponds to the EF in the load displacement diagram. The specimen is loaded from F to H such that the ΔJ evaluated from the area under GHN is equal to the ΔJ calculated in the previous cycle. This process has been continued for 20 cycles

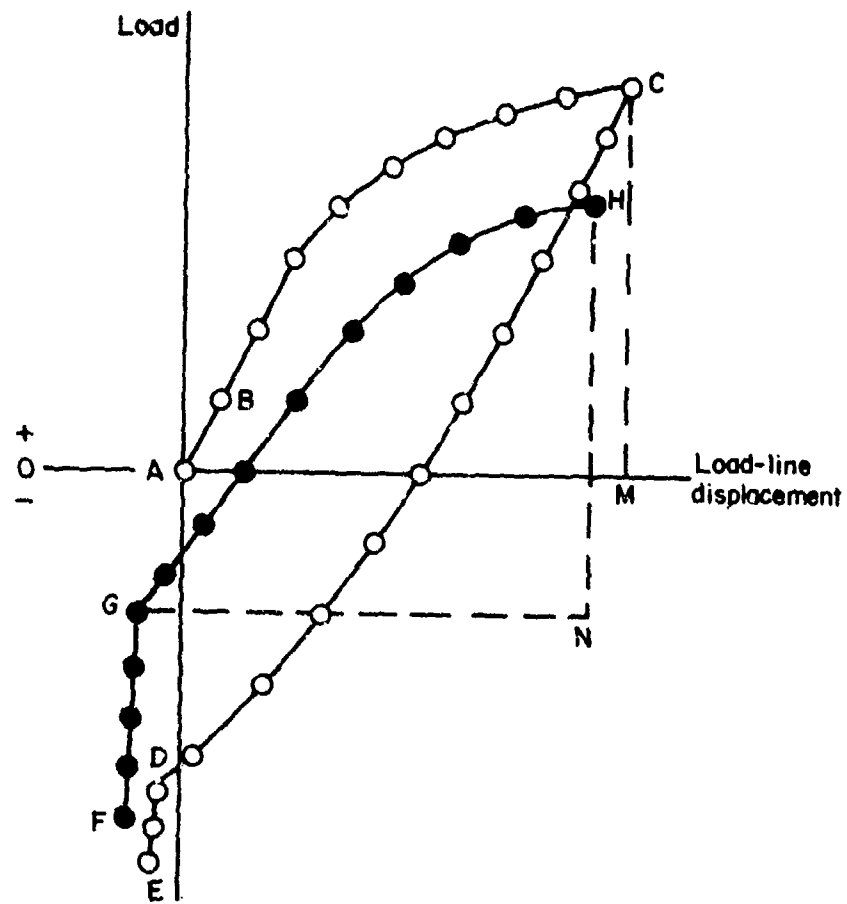


Figure 26. Schematic Representation of Initial Loading Cycles (Reference 81).

and the specimen was broken open to show the crack growth process. Marschall, et al. results indicate that the crack growth rate results from the tests with compressive hold-time greater than one day can be correlated by the Operational- ΔJ parameter. They also reported that the crack growth rate may not be constant over the entire 20 cycles investigated, but may diminish as the test proceeds. One experimental problem experienced by these investigators was that the crack only advanced in the interior, and not on the surface of their compact specimens.

3.3 OTHER FCGR CORRELATIONS

Only two investigations have been identified which provide parameters which could be considered as alternates to the Operational-J Integral parameter. In the first study, high FCGR behavior for a mild steel was described as a function of the crack opening displacement⁸². The data resulting from this study are presented in Figure 27, where the rate of fatigue crack growth is roughly proportional to $(COD)^2$.

In another study, Sadananda and Shahinian⁷⁴ attempted to use the maximum value of the load-line displacement as a correlation parameter. On the basis of the FCGR correlation described in Figure 28, it appears that correlation is possible. These authors attempted to provide a correlation with this parameter because it is substantially easier to measure than the crack tip opening displacement, especially at high temperatures. The authors note that a one-to-one relationship between the load-line displacement and crack tip opening displacement may not exist when the plastic zone size is large. Sadananda and Shahinian also note that the correlation provided by the load-line displacement parameter results in more data scatter than the correlations resulting from the use of the Operational-J parameter.

3.4 THE METHODOLOGY, THE APPROACHES, AND SOME ISSUES

In the previous subsection the known attempts made to extend fracture-mechanics representation of FCGR in the elastic-plastic regime were presented. Correlation with the Operational ΔJ parameter seems to be the most popular among authors^{25,71-74,78,79,81} elastic-plastic FCGR methodology. As their results suggest, ΔJ has correlated FCGR in the elastic-plastic regime for specimens with different geometries. The correlation is very good and both linear elastic and elastic-plastic data lie in the same scatter band.

One can argue the validity of using ΔJ as the correlating parameter to characterize the FCGR in the elastic-plastic regime, since path independence of the J-integral is derived for a

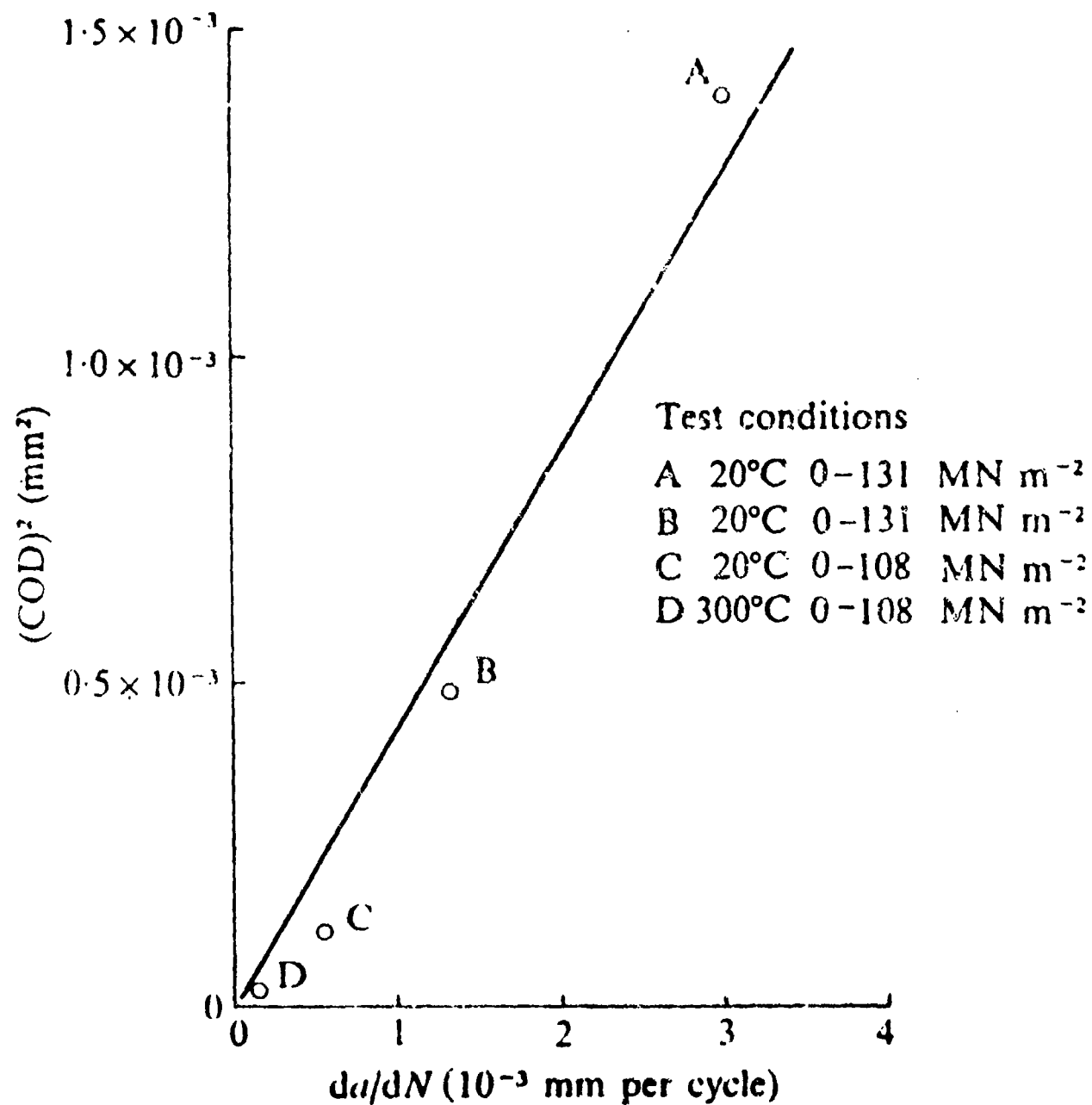


Figure 27. High-Strain Fatigue Crack Propagation Rates as a Function of Crack Opening Displacement, Tests Carried out at 20°C and 300°C in Repeated Tension on Mild Steel Plates 1.83m x 0.91m x 12.7mm Containing a Central Sharp 0.23m slit (Reference 82).

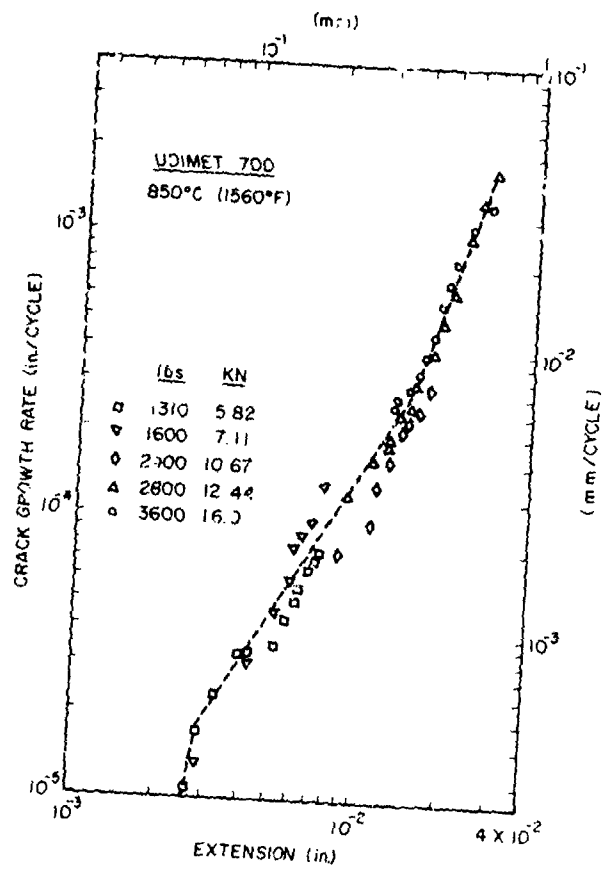


Figure 28. Crack Growth Data in Terms of Load-Line Displacement Parameter (Reference 74).

nonlinear elastic material. When the material undergoes unloading, the mathematical validity of the J-Integral as a parameter which characterizes the nonlinear elastic stresses at the crack tip is violated.

At the high end of the FCGR curve, the crack tip moves forward on each cycle into a relatively undamaged, virgin material in terms of plastic deformation compared to the intense deformation zone at the crack tip. Hence, during the next cycle for which ΔJ is calculated, past history may not be significant compared to loading¹³. It must be noted that the J-Integral is derived for a stationary crack. Figure 21 describes two different ways of defining ΔJ for studying FCGR behavior. To define ΔJ for an actual component, it may require the extensive use of numerical analysis and possibly the contour integral definition of J.

3.4.1 Life Estimation Scheme Using a EPFM Approach

Wilhem et al.⁶² recently presented a modified stress intensity factor approach based on elastic-plastic J-Integral calculations for predicting constant amplitude crack growth lives for cracks growing through nonlinear stress fields established by stress concentrations. Two heat treatment levels, -T651 and -T7351, for the 7075 aluminum alloy were considered. To calculate crack growth lives for thru-thickness cracks, the following steps are taken:

1. Perform a nonlinear analysis of the structure under consideration using finite element analysis, assuming Prandtl-Reuss material behavior.
2. Obtain J_{\max} values for various applied stresses and crack lengths.
3. Compute modified stress intensity factors using

$$K_{I\max} = \begin{cases} \sqrt{\frac{J_{\max} E}{(1-\nu^2)}} & , \text{ plane strain} \\ \text{or} \sqrt{J_{\max} E} & \text{ plane stress} \end{cases} \quad (16)$$

The normalized stress intensity factor $\frac{K_{I\max}}{\sigma_{\max}\sqrt{\pi a}}$, is not merely a function of crack length for a given geometry as in LEFM behavior but also depends on the remotely applied stress above a given stress level.

4. Using $K_{I\max}$ computed via Equation 16, a typical LEFM fatigue crack growth rate description such as Fitzgerald proposes

$$\frac{da}{dN} = C \cdot K_{\max}^m (K_{\max} + K_{\text{env}}) (1-R)^2 \quad (17)$$

can be used to calculate FCGR for a given applied stress cycle.

For the part-thru-crack (PTC) geometries, the authors make the following assumption: the nonlinear effects (or enhancement) for both thru-thickness and PTC geometries will be the same at similar values of the computed elastic stress intensity factor (K_e). For this reason, it is suggested that the (plasticity) modified stress intensity factor (K_p) be written as:

$$K_p = K_e \cdot \phi(\sigma, K_e) \equiv K_e \div \frac{J_e}{J_p} \quad (18)$$

The value of $\phi(\sigma, K_e)$ is a correction to be applied to the elastic stress intensity factors that accounts for the influence of plasticity; it is a function of applied stress (σ), crack length, and the plasticity properties of material, but is assumed independent of geometry. It is not certain at this time whether such an approach will provide better cross correlations than those developed using the LEFM approach modified to account for plasticity via an effective crack length (real length plus plastic zone size).

3.4.2 Summary

Most of the available FCG data generated under the elastic-plastic conditions are presented as:

$$\frac{da}{dN} = f(\Delta J) \quad (19)$$

A limited number of hysteresis loop diagrams and crack length versus number of cycle curves are given in the available literature. Out of this limited information, if numerical methodology

could be developed to calculate other possible parameters, one could test the available data with these parameters.

The data which are available in Dubensky's ⁵ paper are given as

$$\frac{da}{dN} = f (\Delta K) \quad (20)$$

and

$$a = g (N) \quad (21)$$

In this case, as there are no hysteresis loops available, it may be harder to develop numerical techniques to evaluate the ability of other possible parameters which could correlate FCGR data. It is, therefore, suggested that future investigations in the high FCGR regime report displacement parameter information as a function of both cycle and crack length histories, as well as the raw cycle, crack length data.

SECTION IV
RECOMMENDATIONS

Based on the results of the literature review presented in Sections 1 through 3, the following recommendations for additional work are made:

1. Conduct additional FCG data collection studies to determine the specific set of conditions - material, geometrical, and mechanical - for which stress and structural geometry correlations of FCGR by the LEFM parameters fail. Two separate types of studies will be necessary:

- (a) Study FCGR behavior for cracks at high net section stresses
- (b) Study FCGR behavior for small cracks imbedded in a plastic zone at the root of a notch.

2. Define a set of four EPFM parameters for further indepth studies to evaluate their ability for correlating FCGR data. Delineate the advantages and disadvantages of each parameter. The set of EPFM parameters studied should include:

- (a) A LEFM derivative (e.g., $K_{\epsilon} = \epsilon\beta\sqrt{\pi a}$)
- (b) The Operational J ($\Delta J = -\frac{1}{B} \left. \frac{\partial U}{\partial a} \right|_{\delta}$)
- (c) The Crack Tip Opening Displacement, δ_t
- (d) A process zone parameter (e.g., ϵ_{yy}^t)

REFERENCES

1. Gallagher, J.P., "Estimating Fatigue-Crack Lives for Aircraft: Techniques," Experimental Mechanics, Vol. 16, No. 11, Nov. 1976, pp. 425-433.
2. Paris, P.C., "The Fracture Mechanics Approach to Fatigue," Fatigue, An Interdisciplinary Approach, ed. J.J. Burke, N.L. Reed, and V. Weiss, Syracuse University Press, 1964, pp. 107-132.
3. Barsom, J.M., "The Dependence of Fatigue Crack Propagation on Strain Energy Release Rate and Crack Opening Displacement," Damage Tolerance in Aircraft Structures, ASTM STP 486, 1971, pp. 1-15.
4. Frost, N.E., Marsh, K.J., and Pook, L.P., Metal Fatigue, Oxford University Press, Ely House, London, England, 1974.
5. Dubensky, R.G., Fatigue Crack Propagation in 2024-T3 and 7075-T6 Aluminum Alloys at High Stresses, NASA CR-1732, prepared by University of Akron, Ohio, March 1971.
6. Dowling, N.E. and Walker, H., "Fatigue Crack Growth Rate Testing of Two Structural Steels," SAE Paper No. 790459, Presentation at the Society of Automotive Engineers Meetings, Detroit, Michigan, 26 Feb.-2 Mar. 1979.
7. Hammouda, M.M. and Miller, K.J., "Elastic-Plastic Fracture Mechanics Analysis of Notches," Elastic-Plastic Fracture, ASTM STP 668, 1979, pp. 703-719.
8. El Haddad, M.H., Smith, K.N., and Topper, T.H., "Fatigue Crack Propagation of Short Cracks," ASME Transactions, Vol. 101, J. of Engr. Materials and Technology, Jan. 1979, pp. 42-46.
9. Rolfe, S.T. and Barsom, J.M., Fracture and Fatigue Control in Structures, Applications of Fracture Mechanics, Prentice Hall, Inc., Englewood Cliffs, New Jersey, 1977.
10. Westergaard, H.M., "Bearing Pressures and Cracks," Transactions, ASME, Journal of Applied Mechanics, 1939.
11. Irwin, G.R., "Analysis of Stress and Strains Near the End of a Crack Traversing a Plate," Transactions, ASME, Journal of Applied Mechanics, Vol. 24, 1957.
12. Irwin, G.R., "Plastic Zone Near a Crack and Fracture Toughness," 1960 Sagamore Ordnance Materials Conference, Syracuse University, 1961.

13. Paris, P.C., "Fracture Mechanics in the Elastic-Plastic Regime," Flow Growth and Fracture, ASTM STP 631, American Society for Testing and Materials, 1977, pp. 3-27.
14. Dugdale, D.S., "Yielding of Steel Sheets Containing Slits," Journal of Mechanics of Physics of Solids, Vol. 8, 1960.
15. Newman, J.C. Jr., "Fracture of Cracked Plates Under Plane Stress," Int. Journal of Engineering Fracture Mechanics, Vol. 1, No. 1, 1963.
16. Hult, J.A.H. and McClintock, F.A., "Elastic-Plastic Stress and Strain Distribution Around Sharp Notches Under Repeated Shear," 9th Int. Cong. of Appl. Mech., University of Brussels, Vol. 8, 1957, pp. 51-58.
17. Koskinen, M.F., "Elastic-Plastic Deformation of a Single Grooved Flat Plate Under Longitudinal Shear," J. of Basic Eng., Trans. ASME, Vol. 86, Series D, 1963, pp. 585-588.
18. Hutchinson, J.W., "Plastic Stress and Strain Fields at the Crack Tip," Journal of Mechanics and Physics of Solids, 1968, pp. 13-31; pp. 337-347.
19. Rice, J.R., and Rosengren, G.F., "Plane Strain Deformation Near a Crack Tip in Power-Law Hardening Material," Journal of Mechanics and Physics and Solids, 1968, pp: 1-12.
20. Rice, J.R., "A Path Independent Integral and the Approximate Analysis of Strain Concentration by Notches and Cracks," J. of Appl. Mech., Vol. 35, 1968, pp. 379-386.
21. Rice, J.R. and Tracey, D.M., "Computational Fracture Mechanics," Numerical and Computer Methods in Structural Mechanics (Ed. S.J. Fenves et al.), Academic Press, N.Y., 1973, pp. 585-623.
22. Shih, C.F., and Kumar, V., Estimation Technique for the Prediction of Elastic-Plastic Fracture of Structural Components of Nuclear Systems, General Electric Co., Corporate Research and Development, Schenectady, N.Y., Progress Report on Contract RP 1237-1, June 1, 1979.
23. Shih, C.F., Relationship Between the J-Integral and the Crack Opening Displacement for Stationary and Extending Cracks, General Electric Co. TIS Report No. 79CRD075, April 1979.
24. Rice, J.R., "Elastic-Plastic Fracture Mechanics," The Mechanics of Fracture, F. Erdogan, Applied Mechanics Division, American Society of Mechanical Engineers, Vol. 19, 1976, pp. 23-53.

25. Dowling, N.E., and Begley, J.A., "Fatigue Crack Growth During Gross Plasticity and the J-Integral," Mechanics of Crack Growth, ASTM STP 590, American Society for Testing and Materials, 1976, pp. 82-103.
26. Parks, D.M., "Reversed Plasticity from Unloading," Remarks presented at Conference on Elastic-Plastic Mechanics held at Washington University, St. Louis Mo., 31 May-2 June 1978.
27. McClintock, F.A., "On the Plasticity of the Growth of Fatigue Cracks," Fracture of Solids, ed. D.C. Drucker and Gilman, J. Wiley and Sons, N.Y., N.Y., 1963, pp. 65-102.
28. Weiss, V., "Analysis of Crack Propagation in Strain Cycling Fatigue," Fatigue-An Interdisciplinary Approach, ed. Burke, Reed and Weiss, Syracuse University Press, 1964, pp. 179-186.
29. Newman, J.C., Jr., "Finite-Element Analysis of Crack Growth Under Monotonic and Cyclic Loading," Cyclic Stress-Strain and Plastic Deformation Aspects of Fatigue Crack Growth, ASTM STP 637, American Society for Testing and Materials, 1977, pp. 56-80.
30. Liu, H.W. and Iino, N., "A Mechanical Model for Fatigue Crack Propagation," Proceedings of the 2nd International Conference on Fracture, Paper No. 71, Chapman and Hall, 1969, pp. 812-823.
31. Majumdar, S., and Morrow, J., "Correlation Between Fatigue Crack Propagation and Low Cycle Fatigue Properties," Fracture Toughness and Slow-Stable Cracking, ASTM STP 559, American Society for Testing and Materials, 1974, pp. 159-182.
32. Kaisand, L.R., and Mowbray, D.F., "Relationships Between Low-Cycle Fatigue and Fatigue Crack Growth Rate Properties," J. of Testing and Evaluation, Vol. 7, No. 5, Sept. 1979, pp. 270-280.
33. Hu, W. and Liu, H.W., "Crack Tip Strain-A Comparison of Finite Element Method Calculations and Moiré Measurements," Cracks and Fracture, ASTM STP 601, American Society for Testing and Materials, 1976, pp. 522-534.
34. Liu, H.W., Yang, C.Y., and Kuo, A.S., "Cyclic Crack Growth Analyses and Modeling of Crack Tip Deformation," Fracture Mechanics, Ed. Perrone, Liebowitz, Mulville, and Pilkey, University of Virginia, Charlottesville, Va. 1978, pp. 629-647.
35. Elber, W., "The Significance of Fatigue Crack Closure," Damage Tolerance in Aircraft Structures, ASTM STP-486, American Society for Testing and Materials, 1971, pp. 230-242.

36. Rice J.R., "Elastic-Plastic Models for Stable Crack Growth," Mechanics and Mechanism of Crack Growth (Proceedings, Conference at Cambridge, England, April 1973), M.J. May, Ed., British Steel Corporation Physical Metallurgy Center Publication, 1975, pp. 14-39.
37. Chitaley, A.D., and McClintock, F.A., "Elastic-Plastic Mechanics of Steady Crack Growth Under Anti-Plane Shear," Journal of the Mechanics and Physics of Solids, Vol. 19, 1971, pp. 147-163.
38. Amazigo, J.C., and Hutchinson, J.W., "Crack-Tip Fields in Steady Crack Growth with Linear Strain-Hardening," Journal of the Mechanics and Physics of Solids, Vol. 25, 1977, pp. 81-97.
39. Shih, C.F., deLorenzi, H.G., and Andrews, W.R., "Studies on Crack Initiation and Stable Crack Growth," Elastic-Plastic Fracture, ASTM STP 668, J.D. Landes, J.A. Begley, and G.A. Clarke, Eds., American Society for Testing and Materials, 1979, pp. 65-120.
40. Kanninen, M.F., et al., "Elastic-Plastic Fracture Mechanics for Two-Dimensional Stable Crack Growth and Instability Problems," Elastic-Plastic Fracture, ASTM STP 688, American Society for Testing and Materials, 1979, pp. 121-150.
41. Rice, J.R., "An Examination of the Fracture Mechanics Energy Balance From the Point of View of Continuum Mechanics," Proc. 1st International Congress on Fracture, (Ed. T. Yokobori et al.), Japanese Society for Strength and Fracture, Tokyo, Vol. I, 1966, pp. 309.
42. Kfourri, A.P., and Miller, K.J., "Stress, Displacement, Line Integral and Closure Energy Determinations of Crack Tip Stress Intensity Factors," International Journal of Pressure Vessels and Piping, Vol. 2, 1970, pp. 179-191.
43. Kfourri, A.P., and Miller, K.J., "Crack Separation Energy Rate: Elastic-Plastic Fracture Mechanics," Proc. of the Institution of Mech. Engr., London, Vol. 190, 1976, pp. 571-584.
44. Green, G., and Knott, J.F., "The Initiation and Propagation of Ductile Fracture in Low Strength Steels," Journal of Engineering Materials and Technology, Vol. 98, No. 1, January 1976, pp. 37-46.
45. Tong, P. and Pian, T.H.H., "On the Convergence of the Finite Element Method for Problems with Singularity," Int. J. Solids Structures, Vol. 9, 1973, pp. 313-321.
46. Zienkiewicz, O.C., The Finite Element Method in Engineering and Science, McGraw-Hill, London, 1971.
47. Watwood, V.B. Jr., "The Finite Element Method for Prediction of Crack Behavior," Nuclear Eng. and Design, Vol. II, 1969, pp. 323-332.

48. Chan, S.K., Tuba, I.S., and Wilson, W.K., "On the Finite Element Method in Linear Fracture Mechanics," Eng. Fracture Mech., Vol 2, 1970, pp. 1-17.
49. Anderson, G.P., Ruggles, V.L., and Stickor, G.S., "Use of Finite Element Computer Programs in Fracture Mechanics," Int. J. of Fracture Mech., Vol. 7, 1971, pp. 63-76.
50. Hilton, P.D. and Sih, G.C., "Applications of the Finite Element Methods to the Calculations of Stress Intensity Factors," Methods of Analysis of Crack Problems (Ed. G.C. Sih), Noordhoff Int. Publishing, London, 1973.
51. Byskov, E., "The Calculation of Stress Intensity Factors Using the Finite Element Method with Crack Elements," Int. J. Fracture Mech., Vol. 6, No. 2, 1970, pp. 159-167.
52. Tracey, D.M., "Finite Element for Deformation of Crack Tip Elastic Stress Intensity Factors," Eng. Fracture Mech., Vol. 3, No. 3, 1971, pp. 255-266.
53. Tracey, D.M. and Cook, T.S., "Analysis of Power Type Singularities Using Finite Elements," Int. J. Num. Methods in Eng., Vol. 11, No. 8, 1977, pp. 1225-1233.
54. Luk, C.H., Assumed Stress Hybrid Finite-Element Method for Fracture Mechanics and Elasto-Plastic Analysis, ASRL TR 170-1, December 1970.
55. Rhee, H.C., Atluri, S.N., Moriga, K., and Pian, T.H.H., "Hybrid Finite Element Procedures for Analysis Through Flaws in Plates in Bending," 4th Int. Conf. of Structural Mech. in Reactor Tech., San Francisco, Calif., Aug. 1977.
56. Atluri, S.N. and Nakagaki, M., "J-Integral Estimates for Strain Hardening Materials in Ductile Fracture Problems," Proc. AIAA/ASME/SAE 17th Structures, Structural Dynamics and Material Conference, Valley Forge, Pa., May 1976.
57. Atluri, S.N., Nakagaki, M., and Chen, W-H., "Fracture Analysis Under Large-Scale Plastic Yielding a Finite Deformation, Embedded Singularity, Elastoplastic Incremental Finite-Element Solution," Flaw Growth and Fracture, ASTM STP 631, 1977, pp. 42-61.
58. McMeeking, R.M., "Finite Deformation Analysis of Crack-Tip Opening in Elastic-Plastic Materials and Implications for Fracture," J. Mech. Phys. Solids, Vol. 25, 1977, pp. 357-381.
59. Barsoum, R.S., "Triangular Quarter-Point Element as Elastic and Perfectly-Plastic Crack Tip Element," Int. J. for Num. Methods in Eng., Vol. II, 1977, pp. 85-98.

60. Wilson, W.K. and Osias, J.R., "A Comparison of Finite Element Solutions for an Elasto-Plastic Crack Problem," Int. J. of Fracture, Vol. 14, 1978, pp. 45-108.
61. Ratwani, M.M., and Wilhem, D.P., Development and Evaluation of Methods of Plane Stress Fracture Analysis, Part III, Application of the Residual Strength Prediction Technique to Complex Aircraft Structure, AFFDL-TR-73-42, Part III, Air Force Flight Dynamics Laboratory, WPAFB, OH, Aug. 1977.
62. Wilhem, D.P., Ratwani, M.M., Carter, J.P., and Fitzgerald, J.H., Nonlinear Fracture Mechanics Analysis of the T-38 Wing Root Radius, NOR-78-79, Northrop Corporation, Aircraft Group, Hawthorne CA, July 1978.
63. Wilhem, D.P., and Ratwani, M.M., "Crack Growth Resistance at Low Stress Intensities," Trans. ASME, Vol. 100, J. of Engr. Materials and Technology, April 1978, pp. 134-137.
64. Ratwani, M.M., and Wilhem, D.P., "Application of Resistance Curves to Residual Strength Prediction," Trans. ASME, Vol. 100, J. of Engr. Materials and Technology, April 1978, pp. 138-143.
65. Wilhem, D.P., and Ratwani, M.M., "Analogy Between Fatigue Crack Growth and Crack Growth Resistance," Accepted for publication in the Journal of Engineering Materials and Technology, Transaction ASME (1978).
66. Dowling, N.E., "Crack Growth During Low-Cycle Fatigue of Smooth Axial Specimens," Cyclic Stress-Strain and Plastic Deformation Aspects of Fatigue Crack Growth, ASTM STP 637, American Society for Testing and Materials, 1977, pp. 97-121.
67. McEvily, A.J., and Boettner, R.C., "On Fatigue Crack Propagation in fcc Metals," Acta Metallurgica, Vol. 11, 1963, pp. 725-744.
68. Kitagawa, H., Takahashi, S., Suh, C.M., and Miyashita, S., "Quantitative Analysis of Fatigue Process Micro-cracks and Slip Lines Under Cyclic Strains," ASTM Symposium on Fatigue Mechanisms, May 1979, Kansas City, MO.
69. Begley, J.A., and Landes, J.D., "The J-Integral as a Fracture Criterion," Fracture Toughness, ASTM STP 514, American Society for Testing and Materials, 1972, pp. 1-23.
70. Landes, J.D., and Begley, J.A., "The Effect of Specimen Geometry on J_{IC} ," Fracture Toughness, ASTM STP 514, American Society for Testing Materials, 1972, pp. 24-39.

71. Dowling, N.E., "Geometric Effects and the J-Integral Approach to Elastic-Plastic Fatigue Crack Growth," Cracks and Fracture, ASTM STP 601, American Society for Testing and Materials, 1976, pp. 19-32.
72. Dowling, N.E., "Crack Growth During Low-Cycle Fatigue of Smooth Axial Specimens," Cyclic Stress-Strain and Plastic Deformation Aspects of Fatigue Crack Growth, ASTM STP 637, American Society for Testing and Materials, 1977, pp. 97-121.
73. Brose, W.R., and Dowling, N.E., "Size Effects on the Fatigue Crack Growth Rate of Type 304 Stainless Steel," Elastic-Plastic Fracture, ASTM STP 668, American Society for Testing and Materials, 1979, pp. 720-735.
74. Sadananda, K., and Shahinian, P., "A Fracture Mechanics Approach to High-Temperature Fatigue Crack Growth in Udimet 700," Engineering Fracture Mechanics, Vol. 11, pp. 73-84.
75. Rivlin, R.S., and Thomas, A.G., "Rupture of Rubber, 1. Characteristic Energy for Tearing," Journal of Polymer Science, Vol. 10, 1953, p. 291.
76. Rice, J.R., Paris, P.C. and Merkle, J.G., "Some Results of J-Integral Analysis and Estimates," Fracture Toughness Testing, STP 536, American Society for Testing and Materials, 1973, pp. 231-245.
77. Merkle, J.G. and Corten, H.T., "A J-Integral Analysis for The Compact Specimen, Considering Axial Force as Well as Bending Effects," J. of Pressure Vessel Technology, Vol. 96, 1974, pp. 286-292.
78. Sadananda, K., and Shahinian, P., "Application of J-Integral to High Temperature Fatigue Crack Growth in Cold Worked Type 316 Stainless Steel," Int. Journal of Fracture, Vol. 15, 1979, pp. R81-R83.
79. Mowbray, D.F., "Use of a Compact-Type Strip Specimen for Fatigue Crack Growth Rate Testing in the High-Rate Regime," Elastic-Plastic Fracture, ASTM STP 668, American Society for Testing and Materials, 1979, pp. 736-752.
80. Bucci, R.J., Paris, P.C., Landes, J.D. and Rice, J.R., "J-Integral Estimation Procedures," Fracture Toughness, Proceedings of 1971 National Symposium on Fracture Mechanics, Part II, ASTM STP 514, American Society for Testing and Materials, 1972, p. 40.

81. Marschall, C.W., Charman, C.M., Hildebrand, J.F. and Rosenfield, A.R., "Elevated Temperature Fatigue Crack Growth Rates Generated in Controlled ΔJ Tests," Ductility and Toughness Considerations in Elevated Temperature Service, The Winter Annual Meeting of ASME, San Francisco, Dec. 10-15, 1978, pp. 247-263.
82. Edmondson, B., Formby, C.L., Jurevics, R., and Stagg, M.S., Second International Conference on fracture, Brighton, Chapman and Hall, London (1969), p. 192.